
1 **ASF1 activation PI3K/AKT pathway regulates sexual and**
2 **asexual development in filamentous ascomycete**

3 **Shi Wang¹, Xiaoman Liu¹, Chenlin Xiong¹, Susu Gao¹, Wenmeng Xu¹, Lili Zhao¹,**
4 **Chunyan Song¹, Zhuang Li^{1*}, Xiuguo Zhang^{1,2*}**

5 ¹Shandong Provincial Key Laboratory for Biology of Vegetable Diseases and Insect
6 Pests, College of Plant Protection, Shandong Agricultural University, Taian, 271018,
7 China.

8 ²College of Life Sciences, Shandong Normal University, Jinan, 250014, China.

9 *Correspondence and requests for materials should be addressed to Z.L & X.G.Z
10 (Email: liz552@126.com, zhxg@sdau.edu.cn, zhxg@sdu.edu.cn).

11 **Abstract**

12 Sexual and asexual reproduction is ubiquitous in eukaryotes. PI3K/AKT signaling
13 pathway can modulate sexual reproduction in mammals. However, this signaling
14 pathway modulating sexual and asexual reproduction in fungi is scarcely understood.
15 SeASF1, a SeH4 chaperone, could manipulate sexual and asexual reproduction of
16 *Stemphylium eturmiunum*. SeDJ-1, screened from *SeΔasf1* transcriptome, was
17 confirmed to regulate sexual and asexual development by RNAi, of which the
18 mechanism was demonstrated by detecting transcriptional levels and protein
19 interactions of SeASF1, SeH4 and SeDJ-1 by qRT-PCR, and Y2H, Co-IP and
20 Pull-down, respectively. SeASF1 coupling SeH4 bound SeDJ-1 to arouse the sexual
21 and asexual activity. In *S. eturmiunum* genome, SeDJ-1 was upstream while SeGSK3
22 was downstream in PI3K/AKT signaling pathway. Moreover, SeDJ-1 interacted with
23 SePI3K or SeGSK3 *in vivo* and *in vitro*. Significantly, SeDJ-1 or SePI3K could
24 effectively stimulate sexual activity alone, but SePI3K could recover the sexual
25 development of SiSeDJ-1. Meanwhile, SeDJ-1-M6 was a critical segment for
26 interaction of SeDJ-1 with SePI3K. SeDJ-1-M6 played a critical role in irritating
27 sexual reproduction in SiSePI3K, which further uncovered the regulated mechanism
28 of SeDJ-1. Summarily, SeASF1 coupling SeH4 motivates SeDJ-1 to arouse SePI3K
29 involved in sexual reproduction. Thus, SeASF1 can activate PI3K/AKT signaling
30 pathway to regulate sexual and asexual development in filamentous ascomycete.

31 **Introduction**

32 Sexual reproduction is the predominant reproductive strategy in eukaryotes (Dacks
33 and Roger, 1999; Ramesh et al., 2005). A series of factors including mating-types

34 (Böhm et al., 2013; Coppin et al., 1997), pheromone components (Bobrowicz et al.,
35 2002; Lin et al., 2011), G proteins (Li et al., 2007; Studt et al., 2013) and velvet
36 proteins (Bayram and Braus, 2012) are involved in sexual reproduction in fungi.
37 MAPK (Mitogen-Activated Protein Kinase) (Bayram et al., 2012; Chen et al., 2002;
38 Saito, 2010), CWI (Cell Wall Integrity) (Teichert et al., 2014; Zhang et al., 2020) or
39 cAMP-PKA (cyclic Adenosine Monophosphate/Protein Kinase A) signaling
40 pathway1 (Dos Reis et al., 2019) is a highly conserved signaling cascade in
41 eukaryotes and is also required for sexual mating in fungi. More than 20 hypotheses
42 have been used to reveal why sexual reproduction is maintained in fungi (de Visser
43 and Elena, 2007; Hadany and Comeron, 2008). However, most of them devoted to
44 maintenance of fungi sexual mating were still remained unclearly. Thus, sexuality in
45 fungi becomes more perplexing yet intriguing facets of biology that is inevitable to
46 breed a series of magical mechanisms.

47 ASF1 is first identified in *Saccharomyces cerevisiae* and carries out an important
48 role for mating type (Le et al., 1997). ASF1, a H3-H4 chaperone, is highly conserved
49 from yeast to mammals and involved in nucleosome assembly/disassembly
50 (Avvakumov et al., 2011; Eitoku et al., 2008; Prado et al., 2004; Min et al., 2020;
51 Sanematsu et al., 2006), normal cell cycle progression (Groth et al., 2007, Sutton et al.,
52 2001), genomic instability along with histone modification (Das et al., 2014; Li et al.,
53 2008; Recht et al., 2006; Yuan et al., 2009), DNA replication, repair, recombination
54 and transcriptional regulation (Mousson et al., 2007). ASF1 has a serious of magic for
55 modulating female reproduction in mice (Messiaen et al., 2016) and requiring for heat
56 stress response and gametogenesis in *Arabidopsis thaliana* (Zhu et al., 2011; Weng et
57 al., 2014; Min et al., 2019). Meanwhile, ASF1 can also manipulate the sexual
58 reproduction in *Sordaria macrospora* effectively (Gesing et al., 2012). Summarily,
59 ASF1 shows a ubiquitous function for regulating sexual development in animals,
60 plants and fungi. However, whether ASF1 can activate a signaling pathway to mediate
61 sexual or asexual development in filamentous ascomycete is barely accepted.

62 DJ-1, named as PARK7, is first reported to associated with Parkinson's disease (PD)
63 (Bonifati et al. 2012) and then verifies to be an oncogene for mediating the regulation
64 of numerous types of cancer (Bai et al., 2012; Chen et al., 2012; Scumaci et al., 2020).
65 DJ-1 is an essential regulator of multiple cellular processes, including anti-oxidative
66 stress, anti-apoptotic effects, and protein degradation (Taira et al., 2004; Mukherjee et
67 al., 2015; Hijioka et al., 2017). As a multifunctional protein, DJ-1 plays a major role

68 in the phosphatidylinositol-3-kinase (PI3K)/AKT signaling pathway (Yang et al.,
69 2005). The PI3K/AKT signaling pathway manipulates a variety of biological
70 processes, including cell differentiation, proliferation, growth, metabolism, survival,
71 genomic stability, protein synthesis, angiogenesis, cancer (Yang et al., 2018;
72 Engelman et al., 2006; Liu et al., 2020; Patra et al., 2019; Zhou et al., 2017), and even
73 inhibition of apoptosis and oxidative stress and regulation of a variety of downstream
74 molecules (Srinivasan et al., 2005; Gong et al., 2018). Significantly, PI3K/AKT
75 signaling pathway can modulate sexual reproduction in mammals (Shao et al., 2019;
76 Fu et al., 2020). However, the role of DJ-1 or ASF1 in connection with DJ-1 mediates
77 this signaling pathway to irritate sexual and asexual reproduction in filamentous
78 ascomycete is hardly understood.

79 *Stemphylium* and its two closely related genera *Alternaria* and *Ulocladium* belong
80 to filamentous ascomycetes (Simmons., 1967). *Stemphylium* was subject to the
81 ascomycete family Pleosporales and Pleosporaceae (Câmara et al., 2002; Simmons,
82 1989). The sexual states of *Stemphylium* and *Alternaria* are *Pleospora* and *Lewia*,
83 respectively (Lucas and Webster, 1964; Simmons, 1969, 1989; Inderbitzin et al.,
84 2005), but the sexual state of *Ulocladium* has no yet been identified (Wang et al.,
85 2017). Most species within these three similar genera are mainly allied to asexual
86 states (Woudenberg et al., 2013, 2017; Câmara et al., 2002). The taxonomic study of
87 them are mainly focused on asexual means. Until now, very few asexual species of
88 them are corresponding to sexual type, which is still challenged due to lack of
89 understanding the mechanisms of these states.

90 In this study, we investigated the biological function of SeASF1 for regulating
91 sexual and asexual development in *S. eturmiunum*. We showed that SeASF1,
92 identified from *S. eturmiunum*, could modulate sexual development in *S. macrospora*
93 by heterologous expression analysis and was equipped to activate sexual and asexual
94 reproduction in *S. eturmiunum*. A variety of up-regulated or down-regulated genes,
95 including Se02026 (SeDJ-1, unidentified protein), Se01950 (Heat shock protein),
96 Se03485 (LysM domain-containing protein), Se04320 (Proline dehydrogenase),
97 Se07693 (vesicle coat complex COPII, subunit SEC31), Se10206 (Allantoate
98 permease) and Se10302 (Choline dehydrogenase), were identified by comparative
99 analysis of transcriptome data. As a result, Se02026 (SeDJ-1) exhibited a unique
100 characteristic for carrying out sexual and asexual development of *S. eturmiunum* by
101 gene silencing. Subsequently, our experiments demonstrated that SeDJ-1 could

102 directly interact with SeASF1 and SeH4 or with SePI3K and SeGSK3 in PI3K/AKT
103 pathway *in vivo* and *in vitro*, respectively. Furthermore, seven truncations of *Sedj-1*
104 (*Sedj-1-M1*, *Sedj-1-M2*, *Sedj-1-M3*, *Sedj-1-M4*, *Sedj-1-M5*, *Sedj-1-M6* and
105 *Sedj-1-M7*) were obtained and confirmed that *Sedj-1-M6* was a key domain for
106 modulating *Sedj-1* interaction with SePI3K. At the same time, *Sedj-1-M6* was further
107 confirmed to play a crucial role in triggering SePI3K to modulate sexual features
108 contrast to *Sedj-1-M7*. Meanwhile, our study verified that *Sepi3k* could motivate
109 sexual reproduction in *SiSedj-1* strains reversely. In summary, SeASF1 could bind
110 with SeDJ-1 to irritate SePI3K for modulating sexual and asexual reproduction. Thus,
111 PI3K/AKT pathway is assumed to involve in sexual and asexual development in
112 filamentous ascomycetes.
113

114 **Results**

115 **Identification and characterization of ASF1 gene in *S. eturmiunum***

116 ASF1 was identified from *S. eturmiunum* genome database (unpublished) by PCR
117 amplification. Primers for PCR were designed by Primer express 3.0 software
118 (Supplemental Table S2). This gene was named as *Seasfl* (KX033515). SeASF1 has
119 291 amino acids with a calculated molecular mass of 31.98 kDa. Alignment of
120 SeASF1 sequence with its homologous sequences from plants, animals and other
121 fungi species (<https://www.ncbi.nlm.nih.gov/>) (Supplemental Table S1) revealed that
122 the N-terminus sequences (1-154 aa) of ASF1 was highly conserved and contained the
123 ASF1 hist chap superfamily functional domain, but the C-terminus was diversity
124 (Supplemental Figure S2). Phylogenetically, all these analyzed sequences were
125 grouped into three clusters that were labeled by different background colors. The
126 cluster1 was divided into three subclusters with different background colors. Also,
127 SeASF1 shared 98.28% similarity with ASF1 of *S. lycopersici* (KNG47682), and
128 90.51% to 91.13% similarity with ASF1 of two *Pyrenophora* species (XP_003295297
129 and XP_001936595). Notably, SeASF1 shared 92.78% identify with ASF1 of
130 *Setosphaeria turcica* (XP_008022755), and more than 91% identify with ASF1 of
131 five *Bipolaris* species (XP_007710420, XP_007695597, XP_014075349,
132 XP_014554985 and XP_007689798), respectively. However, SeASF1 shared 45.45%
133 similarity with ASF1 of *Schizosaccharomyces pombe* (CAA20365) (Supplemental
134 Figure S1). All these data indicate that ASF1 is widely distributed in eukaryotic
135 organisms.

136 **SeASF1 restores the phenotype of sexual reproduction in *SmΔasf1* mutant**

137 In previous study, the *S. macrospora* ASF1 (XP003345657) was localized to the
138 nucleus and essential for sexual reproduction (Gesing et al., 2012). Alignment of
139 SeASF1 sequence with its homologous sequences from plants, animals, and other
140 fungi species showed that ASF1 has a specifically conserved function domain
141 (Supplemental Figure S2), we doubted whether *Seasfl* operates a similar
142 conservatively function. Here, we heterologously expressed the *S. eturmiunum asf1* in
143 the *SmΔasf1* mutant, and obtained two heterologous expression transformants which
144 were succeeded in complementing the developmental defects of *SmΔasf1* strain
145 (Supplemental Figure S3A). Two transformants, *SmΔasf1::GFPSeasfl-1/2*, were
146 expressed by fusion constructs that were identified by PCR and western blot,

147 respectively (Supplemental Figure S4) (The primal PCR result is shown in
148 Supplemental Figure S23, and the primal western blots results are shown in
149 Supplemental Figure S24, S25). Sexual reproduction of these two transformants was
150 completed after growing on CM medium for 10 days, and perithecia carrying mature
151 asci after inducing for 20 days (Supplemental Figure S3B). Fluorescence microscope
152 showed that *Seasfl* was also localized to the nucleus in *S. macrospore* (Supplemental
153 Figure S3C). Taken together, heterologous expression analyses verify that SeASF1
154 has a conserved function, as well as SmASF1, for producing sexual reproduction in
155 filamentous fungi.

156 **SeASF1 modulates asexual and sexual development in *S. eturmiunum***

157 To uncover the biological functions of the SeASF1 during vegetative and sexual
158 development of *S. eturmiunum*, we obtained two *SeΔasfl* mutant strains:
159 *SeΔasfl-0::EGFP* and *SeΔasfl-5::EGFP*, and two complemented transformants:
160 *SeΔasfl-0::EGFPSeasfl* and *SeΔasfl-5::EGFPSeasfl*. Two knockout mutants were
161 detected by southern blot and PCR (Supplemental Figure S5B, C) (The primal PCR
162 results are shown in Supplemental Figure S26, S27, and the primal southern blot
163 result is shown in Supplemental Figure S28). Two complemented transformants were
164 also detected using western blot and PCR (Supplemental Figure S6) (The primal PCR
165 result is shown in Supplemental Figure S29, and the primal western blots results are
166 shown in Supplemental Figure S30, S31). To determine the role of *Seasfl* in hyphal
167 and colonial growth, these four mutants and WT strains were inoculated on PDA
168 medium for 9 days, respectively. The cultures were then photographed after 1 day, 3
169 days, 5 days, 7 days and 9 days (Supplemental Figure S7A). In comparison to WT,
170 two complemented transformants were almost returned to normal growth as well as
171 colonial and hyphal growth (Supplemental Figure S7B, C). However, two *SeΔasfl*
172 strains produced the hyphal fusion, anomalously distributed of nucleus in mycelium,
173 and abnormal conidia which were significantly opposed to those of the complemented
174 transformants and WT strains (Figure 1A-E). These results suggest that *Seasfl* is
175 involved in asexual development of *S. eturmiunum*. On the other hand, microcosmic
176 observations sexual developmental of these four mutants contrast to WT strains
177 showed two complemented transformants and WT strains produced abundant
178 perithecia and normal asci cultured on CM medium after 4 weeks (Figure 1F).
179 Conversely, *SeΔasfl* strains were completely sterile and did not produce perithecia
180 and asci under the same condition (Figure 1G). Furthermore, the expression levels of

181 genes, including mainly G α subunit, MAT1, MAT2, Ste2 and Ste3 involved in
182 MAPK pathway for modulating sexual reproduction, did not change significantly in
183 the two *Se Δ asf1* mutants compared to WT strain (Supplemental Figure S8). These
184 results suggested that SeASF1 might mobilize a new pathway to regulate sexual
185 reproduction in *S. eturmiunum*.
186 **RNA-seq analysis the differentially expressed genes (DEGs) involved in**
187 **regulation of the developmental functions.**

188 The previous results show that *Seasf1* can modulate asexual and sexual development
189 in *S. eturmiunum* and *S. macrospora*. To further search whether other genes are likely
190 to involve in these developmental functions modulating by *Seasf1*, a comparative
191 analysis of genes expression differences was carried out *Se Δ asf1* and WT-sexual,
192 *Se Δ asf1* and WT-vegetative, and WT- sexual and WT- vegetative. As a result, 3716
193 DEGs between *Se Δ asf1* and WT-sexual, of which 2342 genes up-regulated and 1374
194 genes down-regulated. 3023 DEGs between *Se Δ asf1* and WT-vegetative, of which
195 1719 up-regulated and 1304 down-regulated. 3094 DEGs between WT-sexual and
196 WT-vegetative, of which 1343 up-regulated and 1751 down-regulated (Supplemental
197 Figure S9B). A total of 380 DEGs among three transcripts were identified (fold
198 change >2.0, *q*-value <0.005) (Supplemental Figure S9A) and subsequently analyzed
199 by hierarchical clustering (Supplemental Figure S10). Through the comparative
200 analysis of transcriptome data, we speculated that these significantly up-regulated or
201 down-regulated genes might involve in the SeASF1 regulation of sexual and asexual
202 development.

203 To further determine the roles of these up-regulation or down-regulation genes, the
204 histograms of GO enrichment analysis of DEGs are depended on the data of *Se Δ asf1*
205 and WT-vegetative, and *Se Δ asf1* and WT-sexual. GO analyses found that a large
206 number of genes are potentially involved in the process of cellular, secondary
207 metabolites and development, cell part and catalytic activity in the development of *S.*
208 *eturmiunum* (Supplemental Figure S9C, D). Meanwhile, another seven genes
209 including Se02026 (SeDJ-1, unidentified protein), Se01950 (Heat shock protein),
210 Se03485 (LysM domain-containing protein), Se04320 (Proline dehydrogenase),
211 Se07693 (vesicle coat complex COPII, subunit SEC31), Se10206 (Allantoate
212 permease) and Se10302 (Choline dehydrogenase) were predicted to be involved in
213 *Seasf1* practice on asexual and sexual development (Supplemental Table S4). These

214 findings suggest that SeASF1 is likely to confront with other genes to regulate the
215 asexual and sexual development.

216 **SeDJ-1 plays a role in asexual and sexual development**

217 DJ-1 (SeDJ-1) was cloned from *S. eturmiunum*. SeDJ-1 contains 257 amino acids
218 with a calculated molecular mass of 28 kDa. Phylogenetically, SeDJ-1 sequence with
219 its homologous sequences from plants, animals and other fungi species
220 (<https://www.ncbi.nlm.nih.gov/>) (Supplemental Table S5) were grouped into three
221 clusters that were labeled by different background colors. The cluster3 contained all
222 of the DJ-1 sequences from multiple fungi species that was divided into three
223 subclusters. Also, SeDJ-1 shared 93.77% similarity with DJ-1 of *S. lycopersici*
224 (RAR14805), and less than 20% similarity with DJ-1 of all other fungi species
225 (Supplemental Figure S11). Thus, DJ-1 is widely distributed in eukaryote, but SeDJ-1
226 is considerably conserved with DJ-1 of *S. lycopersici*.

227 To further investigate whether each of these selected seven genes are involved in
228 asexual and sexual development in *S. eturmiunum*, we generated two silenced
229 transformants of each gene by *A. tumefaciens* mediated method. Our experiments
230 confirmed that these seven genes excluded Se02026 (SeDJ-1) compromised on
231 asexual and sexual development (Supplemental Figure S13-S18). Two
232 *Sedj-1*-silenced transformants (Si*Sedj-1*-T1 and Si*Sedj-1*-T4) appeared the slow
233 growth rate of colonies related to the control strains (Supplemental Figure S12A, B).
234 Notably, the nuclei were anomalously distributed in mycelia of two silenced
235 transformants (Figure 2A). Conidiogenous cells of the two silenced lines were
236 swollen at the apex or lateral branch, while they had grown to be secondary mycelia at
237 apex or side in the control strains at 7 days. At 13 days, conidiophores and
238 conidiogenous cells were obvious development and paled in two silenced lines, but
239 conidiogenous cells of the control strains appeared swollen at the apex and darkened
240 and conidia were imaged young, solitary, body brown and ellipsoid to cylindrical. At
241 20 days, subglobose and young conidia were pictured in two silenced lines, however,
242 the control strains had produced near mature oblong conidia. For two silenced lines,
243 the mature conidia were not discovered but conidiophores were turned into bead-like
244 which were significantly different from control strains at 30 days (Figure 2B). By
245 contrast, the young and irregular ascogonia were produced in the two silenced strains,
246 while the young protoperithecia could be discovered in the control strains at 13 days.
247 At 25 days, however, immature perithecia did not observe in the two silenced strains

248 which were significantly different from the control strains. Moreover, at 34 days, the
249 two silenced strains did not produce the perithecia, but the near mature perithecia with
250 asci had produced in the control strains. Finally, the mature asci were only pictured in
251 control strains at 45 days (Figure 2C). These results indicate that SeDJ-1 plays a
252 crucial role in asexual and sexual development for *S. eturmiunum*.

253 **SeASF1 interaction with SeH4 or SeDJ-1, and SeH4 interaction with SeDJ-1**

254 To verify whether can occur the interaction between SeASF1 and SeDJ-1, SeDJ-1 and
255 SeH4. Firstly, the transcript levels of *Sedj-1* and *SeH4* were detected in two *SeΔasf1*
256 mutants. The expressions of *Sedj-1* and *Seasf1* were measured in two *SiSeH4* lines,
257 and those of *Seasf1* and *SeH4* examined in two *SiSedj-1* lines. As a result, *Sedj-1* and
258 *SeH4* showed down and up-regulation in two *SeΔasf1* mutants, respectively (Figure
259 3a). At the same time, *Sedj-1* and *Seasf1* displayed down and up-regulation in two
260 *SiSeH4* lines, respectively (Figure 3B), while *Seasf1* and *SeH4* showed
261 down-regulation in two *SiSedj-1* lines, respectively (Figure 3C). Therefore, SeDJ-1
262 was a positive factor for SeASF1 expression. Secondly, Y2H revealed that SeASF1
263 interacted with SeH4 and SeDJ-1, and SeH4 interacted with SeDJ-1 (Supplemental
264 Figure S19A, B). On the basis of GST pull-down, SeASF1 was specifically interacted
265 with SeH4 (Figure 3D) (The primal western blots of input results are shown in
266 Supplemental Figure S32A, S33A and S34A, while the primal western blots of
267 Pull-down results are shown in Supplemental Figure S32B, S33B and S34B), while
268 SeDJ-1 could interact with SeASF1 and SeH4, respectively (Figure 3E) (The primal
269 western blots of input results are shown in Supplemental Figure S35A, S36A and
270 S37A, while the primal western blots of Pull-down results are shown in Supplemental
271 Figure S35B, S36B and S37B). Finally, all those results of the pull-down experiments
272 were further assured by Co-IP assays (Figure 3F, G) (f-left: The primal western blots
273 of input results are shown in Supplemental Figure S38A, S39A and S40A, while the
274 primal western blots of IP results are shown in Supplemental Figure S38B, S39B.
275 f-right: The primal western blots of input results are shown in Supplemental Figure
276 S41A, S42A and S43A, while the primal western blots of IP results are shown in
277 Supplemental Figure S41B, S42B) (g-left: The primal western blots of input results
278 are shown in Supplemental Figure S44A, S45A and S46A, while the primal western
279 blots of IP results are shown in Supplemental Figure S44B, S45B. g-right: The primal
280 western blots of input results are shown in Supplemental Figure S47A, S48A and
281 S49A, while the primal western blots of IP results are shown in Supplemental Figure

282 S47B, S48B). Thus, SeASF1 interacted with SeH4 or SeDJ-1, and SeH4 also
283 interacted with SeDJ-1. Altogether, SeDJ-1 could cooperate with SeASF1 and SeH4
284 to modulate asexual and sexual development of *S. eturmiunum*.

285 **SeDJ-1 is involved in PI3K/AKT signaling pathway and interacts with SePI3K or**
286 **SeGSK3 in *S. eturmiunum***

287 The PI3K/AKT signaling pathway is a classic signaling cascade that regulates cell
288 growth and proliferation by affecting a multitude of complementary downstream
289 pathways. The previous studies revealed that DJ-1 could increase the AKT
290 phosphorylation and activated the PI3K/AKT signaling pathway in human (Yang et
291 al., 2005; Zhang et al., 2016). However, it has rarely been reported in fungi.
292 Accordingly, the expression levels of *Sepi3k* and *Segsk3* were quantified in two
293 Si*Sedj-1* lines. At the same time, two Si*Sepi3k* lines were obtained using RNA
294 interference. The expression levels of *Sedj-1* and *Segsk3* were examined in two
295 Si*Sepi3k* lines. The results showed that the expression levels of *Sepi3k* or *Sedj-1* were
296 down-regulated in two Si*Sedj-1* or two Si*Sepi3k* lines (Figure 4A), while the
297 expression levels of *Segsk3* was up-regulated in two Si*Sedj-1* lines and two Si*Sepi3k*
298 lines, respectively (Figure 4B). Therefore, *Sedj-1*, a developmental activator, was an
299 upstream component of the *Sepi3k* and *Segsk3* modules that lied in the PI3K/AKT
300 signaling pathway of *S. eturmiunum*. To verify whether SeDJ-1 interacted with these
301 two components in PI3K/AKT signaling pathway, Y2H was first used to ascertain
302 SeDJ-1 interaction with SePI3K or SeGSK3 (Supplemental Figure S20).
303 Subsequently, SeDJ-1 was confirmed to interact with SePI3K or SeGSK3 by pull
304 down (Figure 4C) (The primal western blots of input results are shown in
305 Supplemental Figure S50A, S51A, while the primal western blots of Pull-down
306 results are shown in Supplemental Figure S50B, S51B). Finally, the experiments of
307 both Y2H and pull down were further assured by Co-IP assay (Figure 4D) (The
308 primal western blots of input results are shown in Supplemental Figure S52A, S53A
309 and S54A, while the primal western blots of IP results are shown in Supplemental
310 Figure S52B, S53B). All these data suggest that SeDJ-1 could motivate the major
311 components of the PI3K/AKT signaling pathway to involve in this pathway activity in
312 *S. eturmiunum*.

313 **M6 domain of *Sedj-1* recovers *Sepi3k* silenced transformants to produce**
314 **perithecia.**

315 We previously showed that SeDJ-1 interacted with SePI3K or SeGSK3 and involved
316 in the activity of PI3K/AKT signaling pathway. To decide the critical segment of
317 SeDJ-1 carried out all those functions, seven truncations of *Sedj-1* were obtained and
318 tested whether each of them interacts with SePI3K by Y2H and Co-IP. The results
319 determined that *Sedj-1*-M6 was a key domain for modulating *Sedj-1* interaction with
320 SePI3K (Figure 5A, B) (The primal western blots of input results are shown in
321 Supplemental Figure S55A, S56A and S57A, while the primal western blots of IP
322 results are shown in Supplemental Figure S55B, S56B). Subsequently, *Sedj-1*,
323 *Sedj-1*-M6, *Sedj-1*-M7 and *Sepi3k* were overexpressed in *SiSepi3k* strains,
324 respectively. Eight overexpression transformants, *OE**Sedj-1* (T13 and T30),
325 *OE**Sedj-1*-M6 (T5 and T10), *OE**Sedj-1*-M7 (T18 and T26), and *OE**Sepi3k* (T8 and
326 T13), were obtained. Those overexpression transformants were identified by western
327 blot and qRT-PCR (Figure 5D, E) (The primal western blots results are shown in
328 Supplemental Figure S58-S61). As a result, these overexpression strains excluded
329 *OE**Sedj-1*-M7 (T18 and T26) restored the sexual characteristics in *SiSepi3k* strains
330 and produced abundant perithecia (Figure 5C). The asexual characteristics of these
331 eight overexpression transformants and two *SiSepi3k* transformants were unanimous
332 with those of WT strain (Supplemental Figure S22A). The nuclei distributions in
333 mycelia of these transformants were identified with WT strain (Supplemental Figure
334 S22B). All those results indicate that *Sedj-1*-M6 is a key functional domain for
335 modulating sexual features and plays an important role in PI3K/AKT signaling
336 pathway of *S. eturmiunum*.

337 **The sexual reproduction of *SiSedj-1* strains was recovered by overexpressing** 338 ***Sepi3k***

339 In our previous study, *Sedj-1* was confirmed to be a positive regulator for effecting on
340 *Sepi3k* mediated sexual development in upstream of PI3K/AKT signaling pathway,
341 we attempted to evaluate whether *Sepi3k* was likely to a reverse regulator for
342 dedicating to *Sedj-1* modulated sexual states. Accordingly, *Sepi3k* and *Sedj-1* were
343 overexpressed in *SiSedj-1* lines, respectively. Four overexpression transformants,
344 *OE**Sedj-1*-T5, *OE**Sedj-1*-T20, *OE**Sepi3k*-T8, and *OE**Sepi3k*-T12, were generated to
345 investigate the role of *Sepi3k* in *SiSedj-1* strains. Those overexpression transformants
346 were identified by western blot and qRT-PCR (Supplemental Figure S21B, C) (The
347 primal western blots results are shown in Supplemental Figure S62, S63). At 25 days,
348 two *OE**Sepi3k* strains similar to two *OE**Sedj-1* strains produced abundant perithecia

349 subsequently but *SiSedj-1* strains did not (Supplemental Figure S21A). However, the
350 asexual characteristics of these four transformants were unanimous with WT strain
351 (Supplemental Figure S22A). The nuclei distributions in mycelia of these
352 transformants were identified with WT strain (Supplemental Figure S22B). Together,
353 these results support our hypothesis that *Sepi3k* regulates sexual reproduction in
354 *SiSedj-1* strains reversely.
355

356 Discussion

357 ASF1 was widely present in animals, plants and fungi, but whether ASF1 was related
358 with sexual and asexual reproduction in fungi was scarcely understood. The sexual
359 reproduction of few filamentous fungi species had been described (Coppin et al.,
360 1997). *Stemphylium* is an important genus in filamentous fungi, but typical species *S.*
361 *eturmiunum* has only one ASF1 (SeASF1) which has more than 90% identify with
362 ASF1 of *S. lycopersici* and other nine fungi species but shares less than 50%
363 similarity with ASF1 of *S. pombe*. SeASF1 carried out the same localizations and
364 sexual reproduction characters as SmASF1 of *S. macrospora* (Gesing et al., 2012).
365 Moreover, SeASF1 could manipulate sexual and asexual reproduction obviously in *S.*
366 *eturmiunum*, in which transcriptional levels of a serious of genes in MAPK signaling
367 pathway related to sexual reproduction were hardly changed in *SeΔasf1* mutants. Thus,
368 we supposed that SeASF1 was not involved in MAPK signaling pathway related to
369 the fungi sexual mating (Chen et al., 2002; Saito, 2010) and might activate other
370 signaling pathways for sexual mating in filamentous fungi. To further investigate this
371 hypothesis, we performed a transcriptome analysis of *SeΔasf1*, identifying SeDJ-1
372 and other six genes (Supplemental Table 4) as possible candidates for cooperating
373 with SeASF1 to modulate the sexual and asexual development. Also, SeDJ-1 plays a
374 crucial role in sexual and asexual development of *S. eturmiunum* in contrast to other
375 six genes by observing phenotypes of each silenced transformant.

376 Previous studies revealed that DJ-1 was involved in multiple biological functions in
377 mammals (Hijioka et al., 2017; Scumaci et al., 2020; Mencke, 2021; Nakamura et al.,
378 2021). However, DJ-1 regulation of sexual and asexual differentiation in mammals,
379 plants and fungi was poorly understood. Here, we found that SeDJ-1 could involve in
380 sexual and asexual development in *S. eturmiunum*, and further illuminated the
381 mechanisms of SeDJ-1 infiltrating sexual and asexual development. These
382 mechanisms were further supported by transcriptional levels of *Seasf1*, *SeH4*, and
383 *Sedj-1* in knockout or silenced lines along with SeASF1 interaction with SeH4, and
384 SeDJ-1 interaction with SeASF1 or SeH4 *in vivo* and *in vitro*, respectively. Thus, all
385 those results suggested that SeDJ-1 could cooperate with SeASF1 and SeH4 to arouse
386 the sexual and asexual activity.

387 Sufficient evidences proved that DJ-1 was an important component in PI3K/AKT
388 signaling pathway (Yang et al., 2005) and might bind with various other factors in this

389 pathway to activate a variety of attractive biological processes (van der Brug et al.,
390 2008; Vasseur et al., 2012). By contrast, multiple downstream proteins were reported
391 in PI3K/AKT signaling pathway in mammals (Wang et al., 2013; Xu et al., 2020;
392 Sitaram et al., 2009; Vasseur et al., 2009), but one downstream protein GSK3
393 (SeGSK3) was found in PI3K/AKT signaling pathway in *S. eturmiunum*. Significantly,
394 SeGSK3 exhibited up-regulated trends in both *Sedj-1* and *Sepi3k* silenced
395 transformants, while SePI3K and SeDJ-1 showed down-regulation in *Sedj-1* or *Sepi3k*
396 silenced transformants, respectively. SeDJ-1 should be upstream component of the
397 SePI3K and SeGSK3 modules in PI3K/AKT signaling pathway of *S. eturmiunum*.
398 Moreover, SeDJ-1 also interacted with SePI3K or SeGSK3 in *vivo* and *vitro*.
399 Therefore, SeDJ-1 should be a key upstream protein in PI3K/AKT signaling pathway
400 and was expected to activate it to regulate sexual and asexual reproduction.

401 To further investigate whether SeDJ-1 can involve in sexual and asexual
402 reproduction in *S. eturmiunum* and how it does this work. We verified SeDJ-1 and
403 SePI3K could stimulate sexual activity effectively of *S. eturmiunum* in SeDJ-1 or
404 SePI3K silenced strains compared with their overexpression strains, respectively.
405 Meanwhile, SePI3K overexpression in Si*Sedj-1* strains could recover the sexual states
406 of these strains. Thus, SeDJ-1 and SePI3K are not only two important components of
407 the PI3K/AKT signaling pathway, but also carry out the same functions for regulating
408 sexual development in *S. eturmiunum*. SeDJ-1 could interact with SePI3K in our
409 experiments. To further illuminate the mechanism of SeDJ-1 regulating sexual
410 reproduction, the seven truncations of SeDJ-1 were obtained. As a result, SeDJ-1-M6
411 was defined as a critical segment for interaction of SeDJ-1 with SePI3K and was also
412 proved to be an essential segment for sexual reproduction in OE*Sedj-1*-M6 compared
413 with OE*Sedj-1*-M7. Thus, SeDJ-1-M6 plays a critical role in PI3K/AKT signaling
414 pathway for irritating sexual and asexual reproduction in *S. eturmiunum*. A model is
415 shown in Figure6, SeASF1 coupling SeH4 translocated into the nucleus followed by
416 motivating SeDJ-1 to irritate sexual and asexual means and then SeDJ-1 aroused
417 SePI3K to modulate sexual states. Therefore, SeASF1 could activate PI3K/AKT
418 signaling pathway to regulate sexual and asexual differentiation in filamentous fungi.

419 **Materials and methods**

420 **Strains and culture conditions.** *Stemphylium eturmiunum* strain (EGS 29-099) (WT),
421 *Seasfl* knockout mutants (*SeΔasfl*), *Seasfl* complemented transformants

422 (Se Δ asf1::EGFP*Seasf1*), *Seasf1* heterologous expression transformants
423 (Sm Δ asf1::EGFP*Seasf1*), *Sedj-1* silenced transformants (Si*Sedj-1*-T1 and Si*Sedj-1*-T4)
424 and overexpression transformants (OE*Sedj-1* and OE*Sepi3k*) were cultured in the dark
425 condition at 25°C on complete medium (CM), or potato dextrose agar (PDA) medium
426 for mycelial growth assays. For the hyphal growth measure, each of these strains was
427 inoculated and grown for 9 days at 25°C in glass dish containing 20 mL PDA medium.
428 To determine the morphology of conidia and ascospores, all of the strains were grown
429 on PDA or CM medium (casein acid hydrolysate 0.5 g/L, casein enzymatic
430 hydrolysate 0.5 g/L, glucose 10.0 g/L, Ca(NO₃)₂·4H₂O 1.0 g/L, KH₂PO₄ 0.2 g/L,
431 MgSO₄·7H₂O 0.25 g/L, NaCl 0.15 g/L, yeast extract 1.0 g/L, and agar 15.0 g/L) at
432 25°C. *Escherichia coli* DH5 α or *Agrobacterium tumefaciens* AGL-1 was incubated in
433 LB (Luria-Bertani) medium at 37°C or 28°C, respectively (Lennox, 1995).

434 **Cloning and plasmid construction.** Cloning and propagation of recombinant
435 plasmids were done under standard conditions (Sambrook et al., 2001). Deletion of *S.*
436 *eturmiunum asf1* by homologous recombination was achieved as follows. Briefly, the
437 *Seasf1* flanking regions, 1500 bp upstream and 1500 bp downstream of open reading
438 frame, were amplified using primer pairs *Seasf1*-5f/*Seasf1*-5r and *Seasf1*-3f/*Seasf1*-3r,
439 respectively. The sequences of these primers are summarized in Supplemental Table
440 S2. The upstream fragment was inserted into *Seasf1* knockout vector pXEH by
441 *XhoI*/*BglIII*-digested. Then the downstream fragment was inserted into *BamHI*/*XbaI*
442 sites of the vector *Seasf1*-L-pXEH. The vector pXEH carrying a *Hph* resistance
443 cassette was flanked by the *Seasf1* upstream and downstream sequences
444 (Supplemental Figure S5A).

445 For complementation and heterologous expression analysis, *S. eturmiunum asf1* was
446 cloned from *S. eturmiunum* genome (This genome did not upload) with primers
447 *Seasf1*-pHDT-F/*Seasf1*-pHDT-R, and then cloned into eGPF-pHDT vector.
448 Subsequently, recombinant plasmid eGFP-pHDT-*Seasf1* was transformed into the
449 Se Δ asf1 mutants and *S. macrospora* Δ asf1 (Sm Δ asf1) mutants (S90177) by *A.*
450 *tumefaciens* mediated transformation (ATMT) method, respectively
451 (Bernardi-Wenzel et al., 2016). Transformants, resistant to G418, were screened by
452 PCR and western blot.

453 For co-immunoprecipitation (Co-IP) analysis, SeASF1, histone (H3/H4), and SeDJ-1
454 were amplified from *S. eturmiunum* with primers (Supplemental Table S2), and
455 cloned into the pDL2 or pFL7 in yeast (XK125) by recombination approach (Zhou et

456 al., 2011). Recombinant plasmids were then co-transformed into the protoplasts of
457 *Fusarium graminearum* wild-type strain (PH-1). Transformants were also screened by
458 western blot.

459 RNA interference (Zhao et al., 2016) was used for *Sedj-1* silencing. The
460 complementary cDNA fragments from *Sedj-1* (499 bp) was amplified from *S.*
461 *eturmiunum* using primers in Supplemental Table S2 and inserted into vector pCIT
462 that flanked to the intron to form silencing construct, respectively (Zhao et al., 2016).
463 The constructed plasmid pCH-*Sedj-1* was transformed into *S. eturmiunum* strain by *A.*
464 *tumefaciens* mediated transformation (ATMT) method (Bernardi-Wenzel et al., 2016).
465 For overexpression analysis, *S. eturmiunum Sedj-1* and *Sepi3k* gene were cloned from
466 *S. eturmiunum* strain with primers in Supplemental Table S2, and then cloned into
467 eGFP-pHDT vector, respectively. Subsequently, recombinant plasmid
468 eGFP-pHDT-*Sedj-1* or eGFP-pHDT-*Sepi3k* was transformed into the Si*Sepi3k* lines
469 by ATMT method (Bernardi-Wenzel et al., 2016). Overexpression transformants,
470 resistant to G418 were screened by qRT-PCR and western blot.

471 **DNA extraction and Southern blot.** All strains were inoculated in PDA medium and
472 grown at 25°C for 7 days in the dark condition. Genomic DNA was extracted from
473 mycelia by CTAB (Storchova et al., 2000). Southern blot was performed using the
474 DIG High Prime DNA Labeling and Detection Starter kit I according to the
475 manufacturer's instructions (Roche Diagnostics, Mannheim, Germany). The specific
476 sequence was amplified from *Hph* gene using primer pairs (Supplemental Table S2),
477 and it was then produced a DIG-labeled probe for hybridization. Each experiment was
478 repeated at least three times.

479 **RNA extraction and qRT-PCR.** Total RNA was extracted from mycelia of *S.*
480 *eturmiunum* growing in PDB (Potato Dextrose Broth) cultures using the Fungal RNA
481 Kit (OMEGA Biotechnology, USA). Reverse transcription was done using 1 µg of
482 total RNA per 20 µL reaction. SYBR Color qRT-PCR was performed in 20 µL
483 reactions that included 0.4 µg of cDNA, 0.4 µL of gene-specific upstream and
484 downstream primers, 10 µL of 2 × ChamQ SYBR Color qPCR Master Mix (Vazyme)
485 and 5.2 µL of ddH₂O. The qRT-PCR was performed on an ABI QuantStudio™ 6
486 Quantitative Real-Time PCR System (Applied Biosystems) under the following
487 conditions: 95°C for 5 min, 40 cycles at 95°C for 10 s, and 60°C for 30 s to calculate
488 cycle threshold values, followed by a dissociation program of 95°C for 15 s, 60°C for
489 1 min, and 95°C for 15 s to obtain melt curves. Relative expression levels of all above

490 selected genes were determined by qRT-PCR with specific primers listed in the
491 Supplemental Table 2. Changes in the relative expression level of each gene were
492 calculated by the $2^{-\Delta\Delta CT}$ method (Livak and Schmittgen, 2001). The housekeeping
493 gene *Actin* was used as an internal standard in each case. This experiment was
494 repeated at least three times.

495 **Gene transcription.** For total RNA extraction, WT and *Se Δ asf1* strains were grown
496 for 4 days in PDB medium by the Fungal RNA Kit (OMEGA Biotechnology, USA).
497 The eligible mRNA was enriched with magnetic beads with Oligo (dT).
498 Fragmentation buffer was then added to break the mRNA into short fragments. Using
499 mRNA of WT or *Se Δ asf1* as a template, first-strand cDNA was synthesized with
500 random hexamers, then buffer, dNTPs and DNA polymerase I were added to
501 synthesize second-strand cDNA, followed by using AMPure XP beads to purify
502 double-stranded cDNA. Subsequently, the purified double-stranded cDNA was then
503 subjected to end repair, a tail was added and linked to the sequencing adapter, and
504 then AMPure XP beads were used for fragment size selection. Finally, PCR
505 enrichment was performed to obtain a final cDNA library.

506 RNA-Seq analysis of total RNA from the WT and *Se Δ asf1* stains was performed by
507 Illumina HiSeq4000 (Berry Genomics, Beijing). Approximately 300 bp fragments
508 were inserted into every library, in which 100 bp sequences were read. Low-quality
509 raw reads were filtered. Resulting paired-end sequencing reads were aligned and
510 quantified using TopHat and Cufflinks with default parameter values. De novo
511 transcriptome analysis was used to estimate transcript abundance and differential
512 expression. Gene expression was calculated as fragments per kilobase of transcript per
513 million mapped fragments (FPKM).

514 **Gene Ontology.** Enriched terms from gene ontology (GO) Biological Process, KEGG
515 (Kyoto Encyclopedia of Genes and Genomes), Swiss-Prot (A manually annotated and
516 reviewed protein sequence database), PIR (Protein Information Resource) and PRF
517 (Protein Research Foundation) databases were identified using the available tools at
518 FungiDB (Stajich et al., 2012) and Blast2GO v2.5. To characterize the genes
519 identified from the differentially expressed genes (DEGs), the GO-based trend tests
520 were performed using the Fisher's exact test. Fold change > 2.0, *P* value < 0.005 were
521 considered statistically significant.

522 **Yeast two-hybrid.** To test whether SeASF1 and H4 interact with SeDJ-1, Y2H assay
523 was performed according to the Yeast Protocols Handbook (Clontech) using the Y2H

524 Gold yeast reporter strain (Clontech). The *Seasf1*, *SeH4*, *SeH3* and *Sedj-1* were
525 amplified by PCR from the cDNA of the *S. eturmiunum*. Then, PCR products were
526 purified and digested with restriction enzyme. The *Seasf1* or *SeH4* was inserted into
527 pGBKT7 plasmid. The *Sedj-1* or *SeH4* was inserted into pGADT7 plasmid.
528 Recombinants of *Seasf1*-BD and *Sedj-1*-AD, *Seasf1*-BD and *SeH4*-AD, *SeH4*-BD and
529 *Sedj-1*-AD were co-transformed into yeast strain Y2H gold, respectively. The
530 transformants were screened on SD/-Trp/-Leu medium (TaKaRa Bio) at 30°C for 3-5
531 days and assayed for growth on the SD/-Trp/-Leu/-His/-Ade/X- α -gal plates (TaKaRa
532 Bio). Each experiment was repeated at least three times.

533 **Recombinant protein purification and GST pull-down.** The *Seasf1* was cloned into
534 the pET28a vector after adding a 1 \times FLAG tag to the 5'-terminal of *Seasf1* by PCR.
535 The *Sedj-1* was cloned into the pGEX-6P-1 vector. For the expression of
536 Flag-SeASF1-28a and GST-SeDJ-1, the pET28a construct or pGEX-6P-1 construct
537 was transformed into *E. coli* Transetta (DE3) (Transgene, Beijing, China), and cells
538 were grown to OD₆₀₀=0.6-0.8 at 37°C and then induced with 1M IPTG
539 (isopropyl- β -D-thiogalactoside) for 12-16 h at 16°C. The cells were harvested by
540 centrifugation for 5 min at 8000 rpm at 4°C. The Flag-SeASF1-28a protein cells were
541 resuspended in Ni-lysis buffer (30 mM Tris-HCl, 300 mM NaCl, 30 mM Imidazole,
542 pH 7.5) and lysed with a Ultrasonic Cell Disruptor. The lysate was centrifuged for 30
543 min at 14 000 rpm (4°C), and the supernatant was passed over a Ni-affinity column
544 (GE) three times at least. Flag-SeASF1-28a was eluted by Ni-elution buffer (30 mM
545 Tris-HCl, 300 mM NaCl, 6 M Imidazole, pH 7.5). The GST-SeDJ-1 protein cells
546 were resuspended in GST-lysis buffer (50 Mm HEPES, 500 mM NaCl, pH 8.0) and
547 lysed with a Ultrasonic Cell Disruptor. The lysate was centrifuged for 30 min at 14
548 000 rpm (4°C), and the supernatant was passed over a GST-affinity column
549 (glutathione sepharoseTM 4B beads GE Healthcare, Little Chalfont, Buckinghamshire,
550 UK) three times at least. GST-SeDJ-1 was eluted by GST-elution buffer (50 mM
551 HEPES, 500 mM NaCl, 10 mM L-glutathione, pH 8.0). The eluent proteins were
552 mixed with loading buffer, and were verified by SDS-PAGE. For glutathione
553 S-transferase (GST) pull-down in vitro, GST-SeDJ-1 and Flag-SeASF1-28a were
554 expressed in *E. coli* strain BL21 (DE3). Total proteins of GST-SeDJ-1 and
555 Flag-SeASF1-28a were then incubated with 4000 μ L of glutathione sepharoseTM 4B
556 beads at 4°C for 2 h. The supernatant was removed and the beads were washed by
557 GST-lysis buffer three times. Finally, the beads were eluted by GST-elution buffer.

558 Pull-down of GST-SeDJ-1 with Flag-SeASF1-28a was detected using an anti-Flag
559 (Invitrogen). Each experiment was repeated at least three times.

560 **Co-IP.** *F. graminearum* protoplasts were transfected with the indicated combination
561 plasmids and empty construct. Total mycelium proteins of *F. graminearum* were
562 extracted with an extraction buffer [50 mM HEPES, 130 mM NaCl, 10% glycerin,
563 protease inhibitors (25 mM Glycerol phosphate, 1 mM Sodium orthovanada, 100 mM
564 PMSF), pH 7.4]. For FLAG IP, protein extracts were incubated with 30 μ L of
565 Anti-Flag[®] M2 Affinity Gel beads (Sigma-Aldrich) at 4°C for 4 h, The beads were
566 then collected by centrifugation at 3000 \times g and washed five times with a washing
567 buffer (50 mM HEPES, 130 mM NaCl, 10% glycerin, pH 7.4). The bound proteins
568 were eluted from the beads by boiling for 15 min. The beads were collected by
569 centrifugation at 3000 \times g for 2 min. Proteins were separated by 12% SDS-PAGE gels
570 and detected using immunoblotting with a monoclonal α -Flag antibody
571 (Sigma-Aldrich) or a α -GFP antibody (Invitrogen). Membranes were stained with
572 Ponceau solution (CWBIO, China). Each experiment was repeated at least three
573 times.

574 **Western blot.** Protein samples were separated by 12% SDS-PAGE gels at 100 V for
575 3 h in running buffer (25 mM Tris-base, 200 mM Glycine, 0.1% SDS). Gels were
576 transferred to Immobilon[®]-P PVDF membrane for 1.5 h at 230 mA. Membranes were
577 then blocked in 5% non-fat milk in 1 \times TBST (0.02M Tris-base, 0.14M NaCl, pH 7.4)
578 with 0.1% (vol/vol) Tween-20 prior to addition of GFP or FLAG antibodies
579 (Sigma-Aldrich) at 1:5000 dilution and incubated at room temperature for 1-1.5h. The
580 membranes were washed three times with TBST and then were incubated for 1h with
581 a horseradish peroxidase labeled immunoglobulin G (IgG-HRP) secondary antibody
582 (Thermo Fisher Scientific, no. 31430) at 1:7500 dilution. The specific proteins were
583 visualized by using the ECL Chemiluminescence Detection Kit (Vazyme). The
584 images were caught by Tanon-5200 Chemiluminescent Imaging System (Tanon,
585 China). Each experiment was repeated at least three times.

586 **Microscopy.** To observe the morphology of conidia and conidiophores, all the
587 transformants and WT strains were grown in the dark condition at 25°C for 4 weeks
588 on PDA medium by inserting double slides. Microscopic examination of nuclear
589 distributions in mycelia, the transformants and WT strains were stained using
590 4,6-diamidino-2-phenylindole (DAPI). To image the sexual structures including
591 perithecia and asci, all these test strains were cultured on CM medium at 25°C for 6

592 weeks in dark condition. Perithecia were sectioned by using a double-edged blade in a
593 dissecting microscope (Olympus, SZX10). The asci, conidia and conidiophores were
594 all captured with 20 × or 40 × objectives of Olympus microscope (Olympus BX53,
595 Tokyo, Japan) using differential interference contrast (DIC) and fluorescence
596 illumination. Microscopic characters of asexual structures were further determined by
597 measurements of 50 mature conidia and 50 conidiophores. The experiment was
598 repeated at least three times.

599 **Statistical analysis.** Data were analyzed using Systat 12 (Systat Software Inc., San
600 Jose, CA, USA). The data were subjected to one-way analysis of variance (ANOVA).
601 Student's t-test was used for two means, and Duncan's multiple range test of least
602 significant difference (LSD) was used for more than two means. *P* values of 0.05 and
603 0.01 were used as indicated.

604 **Supplemental data**

605 **Supplemental Figure S1.** Phylogenetic analysis of ASF1 sequences from *S.*
606 *eturmiunum* and all other fungi, plants and animals species.

607 **Supplemental Figure S2.** Alignment of SeASF1 sequence with its homologous
608 sequences from other fungi, plants and animals species.

609 **Supplemental Figure S3.** Phenotypic characterization of the *Seasfl* heterologous
610 expression in *SmΔasfl*.

611 **Supplemental Figure S4.** Heterologous expression transformants of *Seasfl* were
612 verified by PCR and western blot.

613 **Supplemental Figure S5.** Deletion of the *Seasfl* gene in *S. eturmiunum*.

614 **Supplemental Figure S6.** Two complemented transformants of *Seasfl* were verified
615 by PCR and western blot contrast to deleted mutants.

616 **Supplemental Figure S7.** Hyphal and colonial growth of *S. eturmiunum asfl* deleted
617 mutants and complemented transformants.

618 **Supplemental Figure S8.** The effect of *Seasfl* on the transcriptional regulation of
619 regulators on sexual reproduction.

620 **Supplemental Figure S9.** Transcriptome analysis of the differentially expressed
621 genes (DEGs) in a *SeΔasfl* mutant compared with WT-vegetative and WT-sexual
622 strains.

623 **Supplemental Figure S10.** Transcriptome analysis of the differentially expressed
624 genes (DEGs) in *SeΔasfl* mutant and two WT strains.

-
- 625 **Supplemental Figure S11.** Phylogenetic analysis of DJ-1 sequences from *S.*
626 *eturmiunum* and all other fungi, plants and animals.
- 627 **Supplemental Figure S12.** The colonial phenotypes of *Sedj-1* silenced transformants.
- 628 **Supplemental Figure S13.** The asexual and sexual development in Se01950 silenced
629 transformants.
- 630 **Supplemental Figure S14.** The asexual and sexual development in Se03485 silenced
631 transformants.
- 632 **Supplemental Figure S15.** The asexual and sexual development in Se04320 silenced
633 transformants.
- 634 **Supplemental Figure S16.** The asexual and sexual development in Se07693 silenced
635 transformants.
- 636 **Supplemental Figure S17.** The asexual and sexual development in Se10206 silenced
637 transformants.
- 638 **Supplemental Figure S18.** The asexual and sexual development in Se10302 silenced
639 transformants.
- 640 **Supplemental Figure S19.** SeASF1 interaction with SeH4 or SeDJ-1 and SeH4
641 interaction with SeDJ-1.
- 642 **Supplemental Figure S20.** SeDJ-1 interaction with SePI3K or SeGSK3.
- 643 **Supplemental Figure S21.** The sexual reproduction of Si*Sedj-1* strains was recovered
644 by overexpressing *Sepi3k*
- 645 **Supplemental Figure S22.** The asexual development of Si*Sepi3k*, and OE*Sedj-1*,
646 OE*Sedj-1*-M6, OE*Sedj-1*-M7 or OE*Sepi3k* in Si*Sepi3k*, and OE*Sedj-1* or OE*Sepi3k* in
647 Si*Sedj-1* transformants.
- 648 **Supplemental Table S1.** The ASF1 genes of *Stemphylium eturmiunum* and other
649 organism species.
- 650 **Supplemental Table S2.** Primers used in this study.
- 651 **Supplemental Table S3.** Plasmids used in this study.
- 652 **Supplemental Table S4.** The differentially expressed genes in Se Δ *asf1* vs
653 WT-sexual.
- 654 **Supplemental Table S5.** The DJ-1 genes of *Stemphylium eturmiunum* and other
655 organism species.
- 656 **Acknowledgements**

657 We thank Minou Nowrousian (Ruhr-Universität Bochum) for providing *S.*
658 *macrospora* strains. We thank Jingze Zhang (Zhejiang University) for transcriptome
659 analysis and Daohong Jiang (Huazhong Agricultural University) for providing the
660 plasmid. This work was supported by grants from the National Natural Science
661 Foundation of China (31230001, U200220015).

662 **Author contributions**

663 S.W., Z.L. and X.G.Z. designed the experiments and wrote the paper. S.W., X.L.,
664 C.X., S.G., W.X., L.Z. and C.S. performed the experiments. S.W., X.L., C.X., S.G.,
665 W.X., Z.L. and X.G.Z. contributed to the data analysis.

666 **Competing interests**

667 The authors declare no competing interests.

668

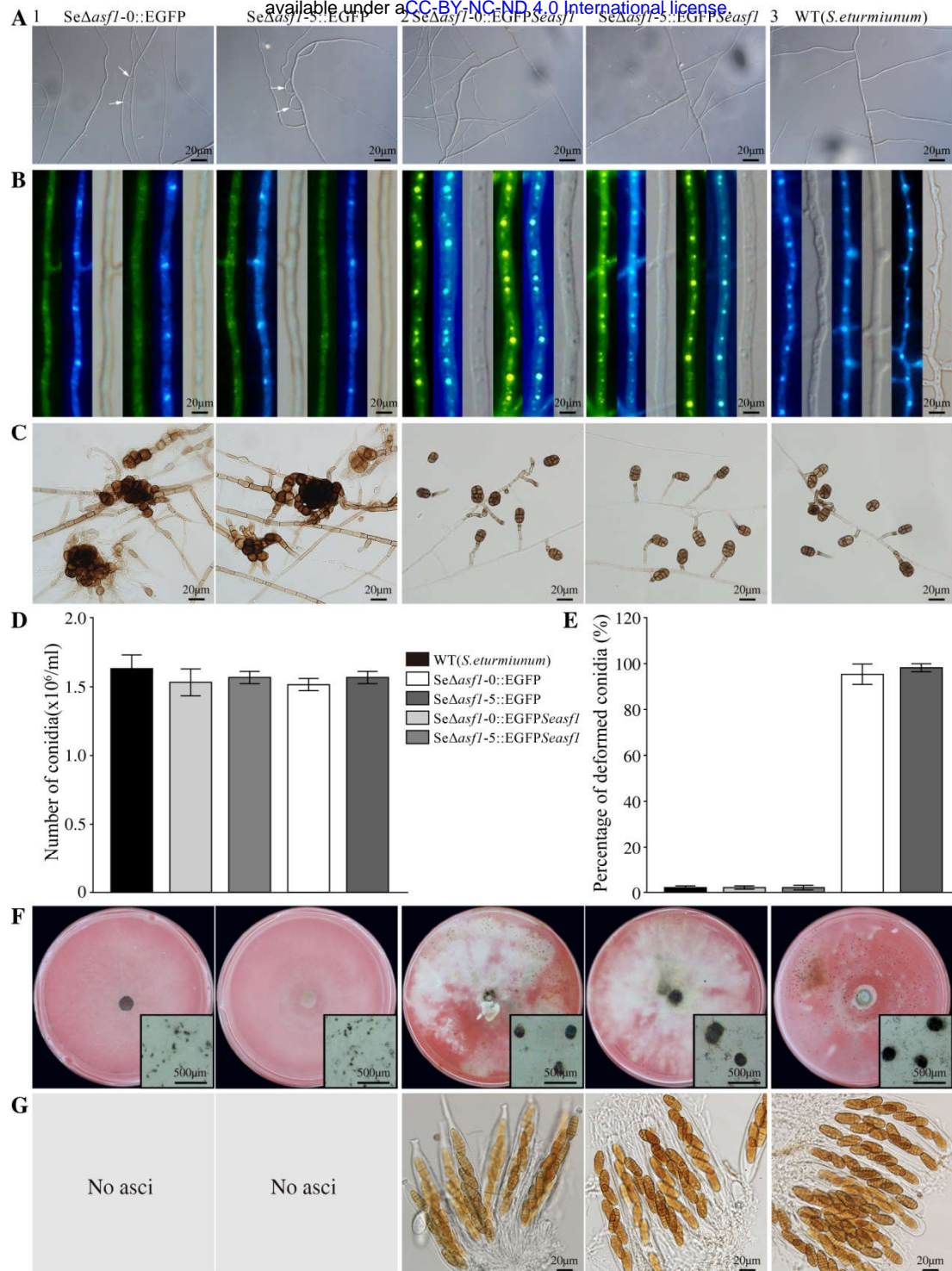


Figure 1 SeASF1 regulates asexual and sexual developmental characterization in *S. eturmiunum*

A, Characterizations of hyphal fusion in two Se Δ asf1 mutants, two Se Δ asf1::EGFPSeasf1 transformants, and WT strains. The images were photographed after growing on PDA medium for 7 days. The fusions in the hyphae were marked with white arrows. **B**, The mycelia of four mutants and WT strains were examined by

DIC and fluorescence microscopy for GFP and DAPI after growing on PDA medium for 12 days. **C**, Conidia morphology of four mutants and WT strains were cultured on CM medium for 4 weeks. Bar= 20 μm . **D**, The number of conidia was counted by blood counting chamber. **E**, Percentage of deformed conidia from two *Se Δ asf1* mutants incubated in CM medium at 4 weeks compared with two *Se Δ asf1::EGFP*Seasf1** mutants and WT strains. **F** and **G**, Perithecia of four mutants and WT strains were visualized as black structures on CM medium. Perithecia were shown in the lower right. **G**, Two *Se Δ asf1* mutants were not able to produce perithecia that were opposed to two *Se Δ asf1::EGFP*Seasf1** mutants and WT strains. Photographs were taken at 6 weeks after sexual induction. Bar= 500 μm .

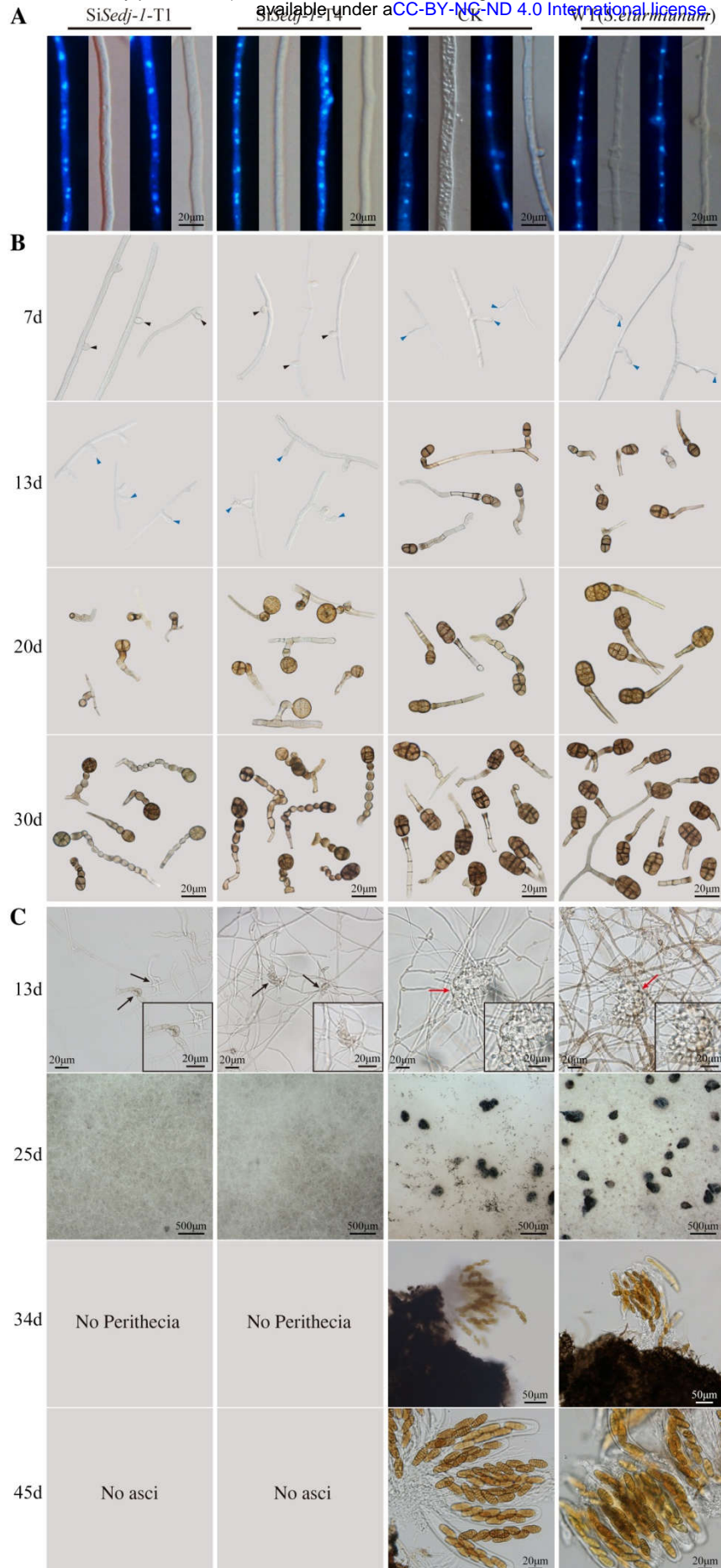


Figure 2 SeDJ-1 plays a role in asexual and sexual development of *S. eturmiunum*

A, The mycelium of two silenced transformants, CK and WT strains were incubated on PDA medium for 6 days and examined by DIC and fluorescence microscopy. Two silenced transformants were Si*Sedj-1*-T1 and Si*Sedj-1*-T4. *S. eturmiunum* and control strains were used as WT and CK, respectively. The nuclei of the mycelia were discovered under the fluorescence microscopy after staining by DAPI. **B**, For the microscopic investigation of conidiophores, conidiogenous cells and conidia development, two silenced transformants, CK and WT strains were grown on CM medium for 7 days, 13 days, 20 days and 30 days, respectively. Black arrowheads indicated conidiogenous cells, and blue arrowheads indicated secondary mycelia. **C**, For the microscopic investigation of ascogonia, protoperithecia, young perithecia and asci development, all strains were grown on PDA medium and examined after growth at 25 °C for 13 days, 25 days, 34 days and 45 days, respectively. Insets showed enlarged ascogonia and protoperithecia on the bottom right sides. Perithecia were visualized as black structures. Black arrows indicated ascogonia, and red arrows indicate protoperithecia. Bar= 20 µm, 50 µm and 500 µm.

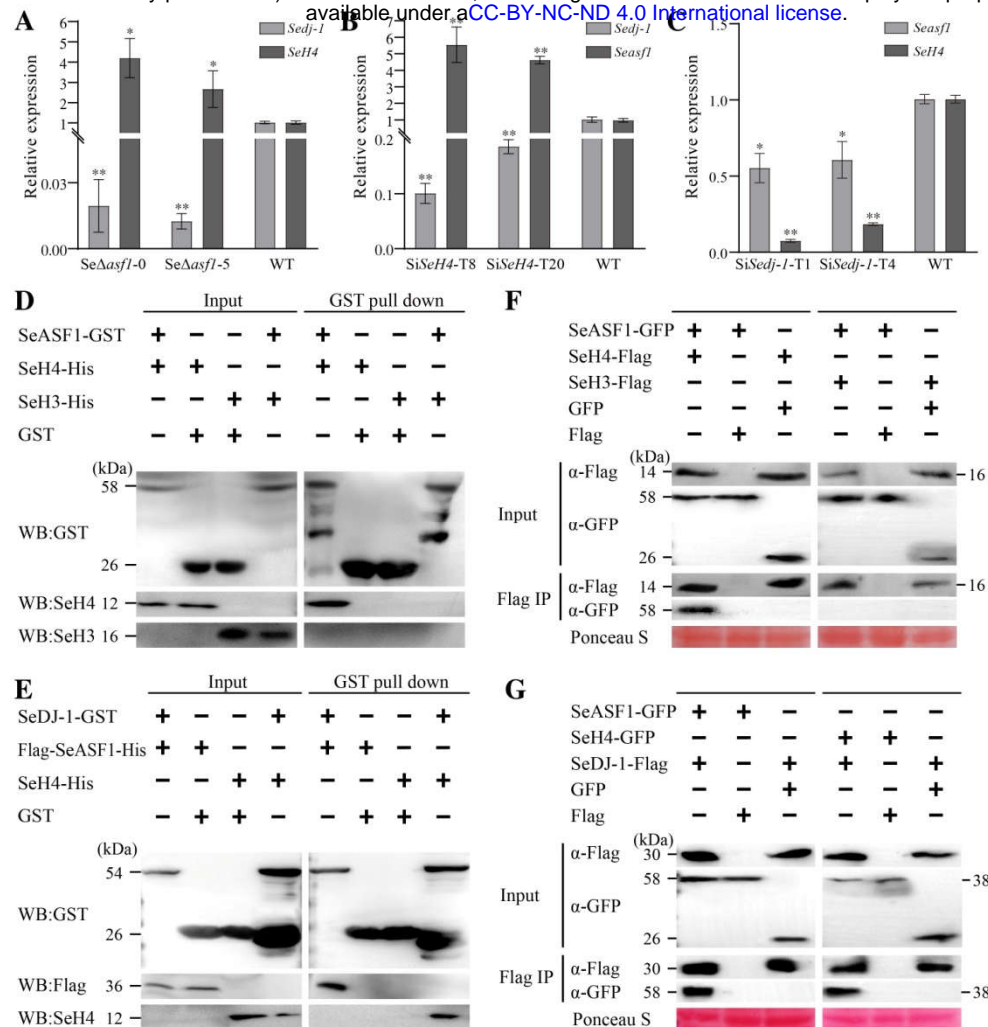


Figure 3 SeASF1 interaction with SeH4 or SeDJ-1, and SeH4 interaction with SeDJ-1

A, The expression levels of *Sedj-1* and *SeH4* in two *Se Δ asf1* mutants were measured by qRT-PCR. **B**, The expression levels of *Sedj-1* and *Seasf1* in two *SiSeH4* lines were measured by qRT-PCR. **C**, The expression levels of *Seasf1* and *SeH4* in two *SiSeDJ-1* lines were measured by qRT-PCR. The degree of WT was assigned to value 1.0. Two *Seasf1* deleted mutants were *Se Δ asf1-0* and *Se Δ asf1-5*. Two *SeH4*-silenced lines were *SiSeH4-T8* and *SiSeH4-T20*. Two *Sedj-1*-silenced lines were *SiSeDJ-1-T1* and *SiSeDJ-1-T4*. *S. eturmiunum Actin* was used as endogenous control. The bars indicated statistically significant differences (ANOVA; * $P < 0.05$, ** $P < 0.01$). **D**, SeASF1 was cloned into plasmid pGEX-6P-1. SeH4 or SeH3 was cloned into plasmid pET28a. SeASF1-GST was expressed in *E. coli* and incubated with SeH4-His or SeH3-His, purified (pull-down) by glutathione sepharose beads. Recombinant GST was control. SeH4-His was pulled down by SeASF1-GST. **E**, SeDJ-1 was cloned into plasmid

pGEX-6P-1. Flag-SeASF1 or SeH4 was cloned into plasmid pET28a. SeH4-His and Flag-SeASF1-His were both retained by SeDJ-1-GST. F, SeASF1 was cloned into plasmid pDL2, SeH4 or SeH3 was cloned into plasmid pFL7. Total proteins were extracted from *F. graminearum* protoplasts expressing SeASF1-GFP, SeH4-Flag, and SeH3-Flag. Recombinant GFP or Flag was control. The immune complexes were immunoprecipitated with α -Flag antibody (α -Flag IP). Coprecipitation of SeH4-Flag or SeH3-Flag was detected by immunoblotting. G, SeH4 was cloned into plasmid pDL2. SeDJ-1 was cloned into plasmid pFL7. Total proteins were extracted from *F. graminearum* protoplasts expressing SeASF1-GFP, SeH4-GFP, and SeDJ-1-Flag. Coprecipitation of SeDJ-1-Flag was detected by immunoblotting. Membranes were stained with Ponceau S to confirm equal loading. Protein sizes are indicated in kDa. Each experiment was repeated at least three times.

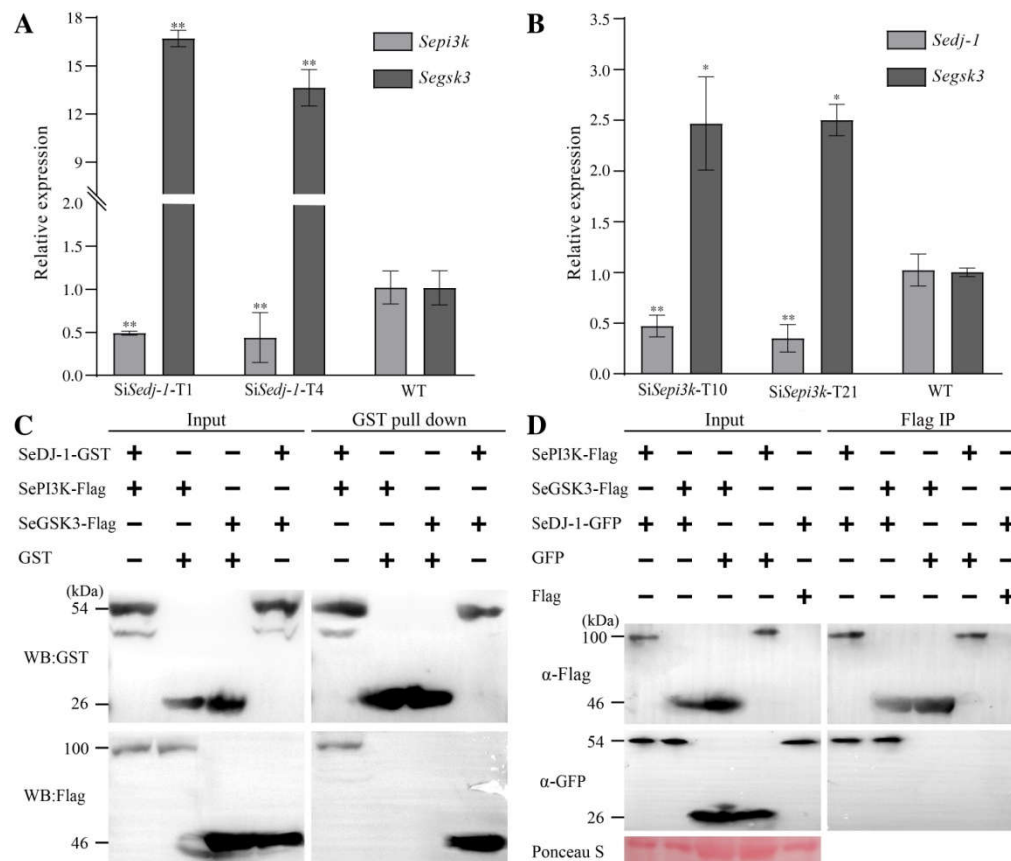


Figure 4 SeDJ-1 is involved in PI3K/AKT signaling pathway and interacts with SePI3K or SeGSK3 in *S. eturmiunum*

A, The expression levels of *Sepi3k* and *Segsk3* in two *Sedj-1* lines were measured by qRT-PCR. **B**, The expression levels of *Sedj-1* and *Segsk3* in two *SiSepi3k* lines were quantified by qRT-PCR. The degree of WT was assigned to value 1.0. Two *Sepi3k*-silenced lines were *SiSepi3k*-T10 and *SiSepi3k*-T21. *S. eturmiunum Actin* was used as

endogenous control. The bars indicated statistically significant differences (ANOVA; $*P < 0.05$, $**P < 0.01$). **C**, SeDJ-1 was cloned into plasmid pGEX-6P-1. Flag-SePI3K or Flag-SeGSK3 was cloned into plasmid pET28a. Recombinant SeDJ-1-GST, Flag-SePI3K-His and Flag-SeGSK3-His were expressed in *E. coli*. SeDJ-1-GST was incubated with Flag-SePI3K-His or Flag-SeGSK3-His and subsequently purified (pull-down) by glutathione sepharose beads. GST-SeDJ-1 was both pulled down Flag-SePI3K-His and Flag-SeGSK3-His. **D**, SeDJ-1 was cloned into plasmid pDL2. SePI3K or SeGSK3 was cloned into plasmid pFL7. Total proteins were extracted from *F. graminearum* protoplasts expressing SeDJ-1-GFP and SePI3K-Flag, SeDJ-1-GFP and SeGSK3-Flag. The immune complexes were immunoprecipitated with α -Flag antibody (α -FLAG IP), and the bound protein was detected by immunoblotting. Membranes were stained with Ponceau S to confirm equal loading. Protein sizes are indicated in kDa. Each experiment was repeated at least three times.

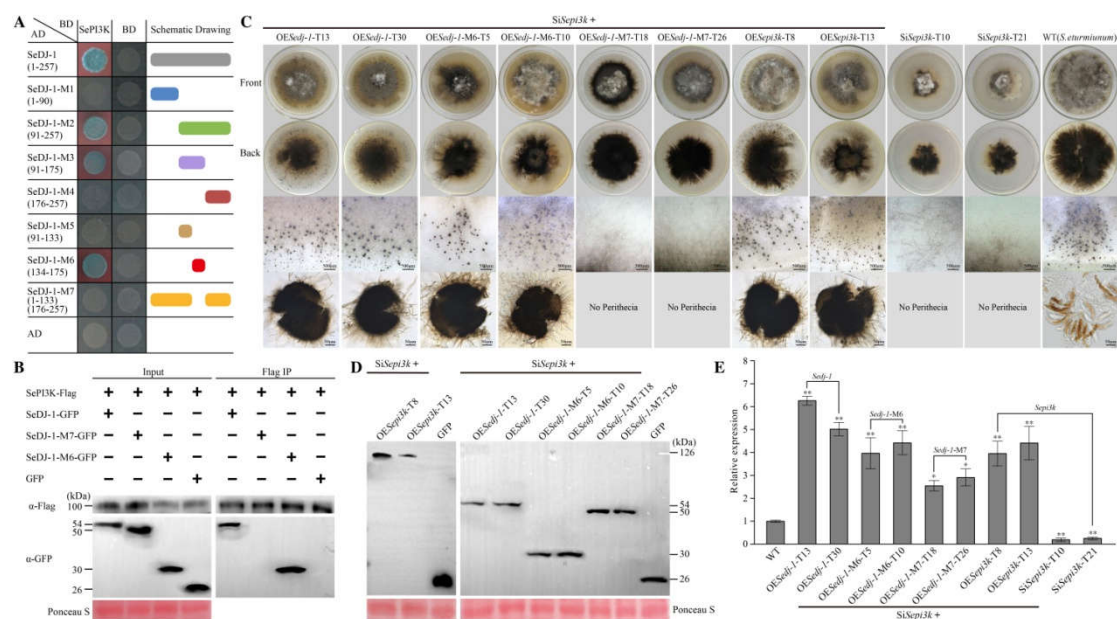


Figure 5 M6 domain of *Sedj-1* induces *Sepi3k* silenced transformants to recover perithecia.

A, Seven truncations of *Sedj-1* interacted with full length SePI3K by Y2H. **B**, SePI3K was cloned into plasmid pFL7. Three selected truncations, SeDJ-1, SeDJ-1-M6 and SeDJ-1-M7, were cloned into plasmid pDL2, respectively. Total proteins were then extracted from *F. graminearum* protoplasts expressing SePI3K-Flag, SeDJ-1-GFP, SeDJ-1-M6-GFP and SeDJ-1-M7-GFP alone. GFP-fusion was used as control. The immune complexes were immunoprecipitated using α -Flag antibody (Flag IP). Coprecipitation of SePI3K-Flag was detected by immunoblotting. **C**, *Sedj-1*, *Sedj-1*-

M6, *Sedj-1-M7* and *Sepi3k* were overexpressed in the *Sepi3k* silenced strains, respectively. Eight overexpression transformants, *OESedj-1* (T13 and T30), *OESedj-1-M6* (T5 and T10), *OESedj-1-M7* (T18 and T26), and *OESepi3k* (T8 and T13), were obtained and cultured on PDA medium for inducing perithecia production. *Sepi3k* silenced and WT strains were used as controls. The images of perithecia were photographed after growing for 30 days. Those overexpression transformants excluded *OESedj-1-M7* (T18 and T26) produced abundant perithecia compared with *SiSepi3k* strains. Bar= 50 μ m and 500 μ m. **D**, Those overexpression transformants were identified by western blot using GFP antibody. **E**, The expression levels of *Sedj-1*, *Sedj-1-M6*, *Sedj-1-M7* and *Sepi3k* within corresponding to overexpression transformants were measured by qRT-PCR related to two *Sepi3k* silenced lines. The degree of WT was assigned to value 1.0. *Actin* gene of *S. eturmiunum* was used as endogenous control. The bars indicated statistically significant differences (ANOVA; * $P < 0.05$, ** $P < 0.01$). Each experiment was repeated at least three times.

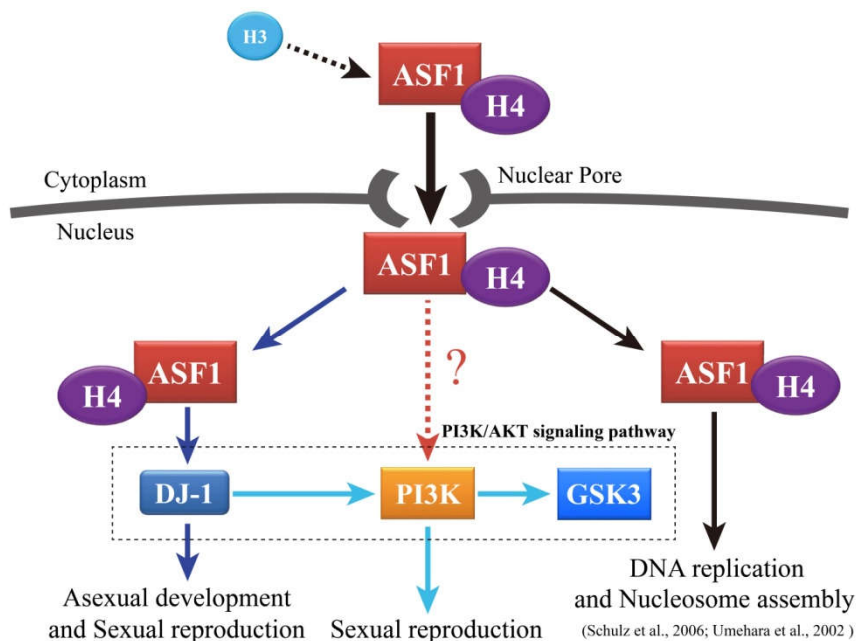


Figure 6 A model for ASF1 binding H4 (ASF1-H4) activates DJ-1 to mediate sexual and asexual reproduction in *S. eturmiunum*

ASF1, a molecular chaperone, interacts with H4 and then translocates into nucleus through the nuclear pore. After getting into nucleus, the dimer of ASF1-H4 modulates DNA replication and nucleosome assembly. ASF1-H4 combines with DJ-1

constituting a new trimeric complex that plays a novel role for modulating sexual and asexual reproduction. Subsequently, DJ-1 also participates in PI3K/AKT signaling pathway for regulating sexual reproduction. Here, it is unknown whether the dimer of ASF1-H4 directly activates PI3K to involve in PI3K/AKT signaling pathway for sexual reproduction process.

Parsed Citations

Arvakumov, N., Nourani, A., and Côté, J. (2011). Histone chaperones: modulators of chromatin marks. *Mol. Cell* 41: 502–514.

Google Scholar: [Author Only Title Only Author and Title](#)

Bai, J., Guo, C., Sun, W., Li, M., Meng, X., Yu, Y., Jin, Y., Tong, D., Geng, J., Huang, Q., et al. (2012). DJ-1 may contribute to metastasis of non-small cell lung cancer. *Mol. Biol. Rep.* 39: 2697–2703.

Google Scholar: [Author Only Title Only Author and Title](#)

Bayram, Ö., and Braus, G.H. (2012). Coordination of secondary metabolism and development in fungi: the velvet family of regulatory proteins. *FEMS Microbiol. Rev.* 36: 1–24.

Google Scholar: [Author Only Title Only Author and Title](#)

Bayram, Ö., Bayram, Ö.S., Ahmed, Y.L., Maruyama, J., Valerius, O., Rizzoli, S.O., Ficner, R., Irniger, S., and Braus, G.H. (2012). The *Aspergillus nidulans* MAPK module AnSte11-Ste50-Ste7-Fus3 controls development and secondary metabolism. *PLoS Genet.* 8: e1002816.

Google Scholar: [Author Only Title Only Author and Title](#)

Bernardi-Wenzel, J., Quecine, M.C., Azevedo, J.L., and Pamphile, J.A. (2016). *Agrobacterium*-mediated transformation of *Fusarium proliferatum*. *Genet. Mol. Res.* 15.

Google Scholar: [Author Only Title Only Author and Title](#)

Bobrowicz, P., Pawlak, R., Correa, A., Bell-Pedersen, D., and Ebbole, D.J. (2002). The *Neurospora crassa* pheromone precursor genes are regulated by the mating type locus and the circadian clock. *Mol. Microbiol.* 45: 795–804.

Google Scholar: [Author Only Title Only Author and Title](#)

Böhm, J., Hoff, B., O’Gorman, C.M., Wolfers, S., Klux, V., Binger, D., Zadra, I., Kürnsteiner, H., Pöggeler, S., Dyer, P.S., et al. (2013). Sexual reproduction and mating-type-mediated strain development in the penicillin-producing fungus *Penicillium chrysogenum*. *Proc. Natl. Acad. Sci. U S A* 110: 1476–1481.

Google Scholar: [Author Only Title Only Author and Title](#)

Bonifati, V., Rizzu, P., van Baren, M.J., Schaap, O., Breedveld, G.J., Krieger, E., Dekker, M.C., Squitieri, F., Ibanez, P., Joosse, M., et al. (2003). Mutations in the DJ-1 gene associated with autosomal recessive early-onset parkinsonism. *Science* 299: 256–259.

Google Scholar: [Author Only Title Only Author and Title](#)

Câmara, M.P.S., O’Neill, N.R., and van Berkum, P. (2002). Phylogeny of *Stemphylium* spp. based on ITS and glyceraldehyde-3-phosphate dehydrogenase gene sequences. *Mycologia* 94: 660–672.

Google Scholar: [Author Only Title Only Author and Title](#)

Chen, J., Chen, J., Lane, S., and Liu, H. (2002). conserved mitogen-activated protein kinase pathway is required for mating in *Candida albicans*. *Mol. Microbiol.* 46: 1335–1344.

Google Scholar: [Author Only Title Only Author and Title](#)

Chen, Y., Kang, M., Lu, W., Guo, Q., Zhang, B., Xie, Q., and Wu, Y. (2012). DJ-1, a novel biomarker and a selected target gene for overcoming chemoresistance in pancreatic cancer. *J. Cancer Res. Clin. Oncol.* 138: 1463–1474.

Google Scholar: [Author Only Title Only Author and Title](#)

Coppin, E., Debuchy, R., Arnais, S., and Picard, M. (1997). Mating types and sexual

Dacks, J., and Roger, A.J., (1999). The first sexual lineage and the relevance of facultative sex. *J. Mol. Evol.* 48: 779–783.

Google Scholar: [Author Only Title Only Author and Title](#)

Das, C., Roy, S., Namjoshi, S., Malarkey, C.S., Jones, D.N., Kutateladze, T.G., Churchill, M.E., and Tyler, J.K. (2014). Binding of the histone chaperone ASF1 to the CBP bromodomain promotes histone acetylation. *Proc. Natl. Acad. Sci. U S A* 111: E1072–1081 (2014).

Google Scholar: [Author Only Title Only Author and Title](#)

de Visser, J. A.G.M., and Elena, S.F. (2007). The evolution of sex: empirical insights into the roles of epistasis and drift. *Nat. Rev. Genet.* 8: 139–149 (2007).

Google Scholar: [Author Only Title Only Author and Title](#)

development in filamentous ascomycetes. *Microbiol. Mol. Biol. Rev.* 61: 411–428.

Google Scholar: [Author Only Title Only Author and Title](#)

Dos Reis, T.F., Mellado, L., Lohmar, J.M., Silva, L.P., Zhou, J.J., Calvo, A.M., Goldman, G.H., and Brown, N.A. (2019). GPCR-mediated glucose sensing system regulates light-dependent fungal development and mycotoxin production. *PLoS Genet.* 15: e1008419.

Google Scholar: [Author Only Title Only Author and Title](#)

Eitoku, M., Sato, L., Senda, T., and Horikoshi, M. (2008). Histone chaperones: 30 years from isolation to elucidation of the mechanisms of nucleosome assembly and disassembly. *Cell. Mol. Life Sci.* 65: 414–444.

Google Scholar: [Author Only Title Only Author and Title](#)

Engelman, J.A., Luo, J., and Cantley, L.C. (2006). The evolution of phosphatidylinositol 3-kinases as regulators of growth and metabolism. *Nat. Rev. Genet.* 7: 606–19.

Google Scholar: [Author Only](#) [Title Only](#) [Author and Title](#)

Fu, G., Dai, J., Li, Z., Chen, F., Liu, L., Yi, L., Teng, Z., Quan, C., Zhang, L., Zhou, T., et al. (2020). The role of STAT3/p53 and PI3K-AKT-mTOR signaling pathway on DEHP-induced reproductive toxicity in pubertal male rat. *Toxicol. Appl. Pharmacol.* 404: 115151.

Google Scholar: [Author Only](#) [Title Only](#) [Author and Title](#)

Gesing, S., Schindler, D., Fränzel, B., Wolters, D., and Nowrousian, M. (2012). The histone chaperone ASF1 is essential for sexual development in the filamentous fungus *Sordaria macrospora*. *Mol. Microbiol.* 84: 748–765.

Google Scholar: [Author Only](#) [Title Only](#) [Author and Title](#)

Gong, J., Zhang, L., Zhang, Q., Li, X., Xia, X.J., Liu, Y.Y., and Yang, Q.S. (2018). Lentiviral vector-mediated SHC3 silencing exacerbates oxidative stress injury in nigral dopamine neurons by regulating the PI3K-AKT-FoxO signaling pathway in rats with parkinson's disease. *Cell. physiol. Biochem.* 49: 971–984.

Google Scholar: [Author Only](#) [Title Only](#) [Author and Title](#)

Groth, A., Corpet, A., Cook, A.J., Roche, D., Bartek, J., Lukas, J., and Almouzni, G. (2007). Regulation of replication fork progression through histone supply and demand. *Science* 318: 1928-1931.

Google Scholar: [Author Only](#) [Title Only](#) [Author and Title](#)

Hadany, L. and Comeron, J.M. (2008). Why are sex and recombination so common? *Ann. N. Y. Acad. Sci.* 1133: 26–43.

Google Scholar: [Author Only](#) [Title Only](#) [Author and Title](#)

Hijioka, M., Inden, M., Yanagisawa, D., and Kitamura, Y. (2017). DJ-1/PARK7: a new therapeutic target for neurodegenerative disorders. *Biol. Pharm. Bull.* 40: 548–552.

Google Scholar: [Author Only](#) [Title Only](#) [Author and Title](#)

Inderbitzin, P., Harkness, J., Turgeon, B.G., and Berbee, M.L. (2005). Lateral transfer of mating system in *Stemphylium*. *Proc. Natl. Acad. Sci. U S A* 102: 11390–11395.

Google Scholar: [Author Only](#) [Title Only](#) [Author and Title](#)

Le, S., Davis, C., Konopka, J.B., and Sternglanz, R. (1997). Two new S-phase-specific genes from *Saccharomyces cerevisiae*. *Yeast* 13: 1029–1042.

Google Scholar: [Author Only](#) [Title Only](#) [Author and Title](#)

Lennox, E.S. (1955). Transduction of linked genetic characters of the host by bacteriophage P1. *Virology* 1: 190-206.

Google Scholar: [Author Only](#) [Title Only](#) [Author and Title](#)

Li, L., Wright, S.J., Krystofova, S., Park, G., and Borkovich, K.A. (2007). Heterotrimeric G protein signaling in filamentous fungi. *Annu. Rev. Microbiol.* 61: 423–452.

Google Scholar: [Author Only](#) [Title Only](#) [Author and Title](#)

Li, Q., Zhou, H., Wurtele, H., Davies, B., Horazdovsky, B., Verreault, A., and Zhang, Z. (2008). Acetylation of histone H3 lysine 56 regulates replication-coupled nucleosome assembly. *Cell* 134: 244–255.

Google Scholar: [Author Only](#) [Title Only](#) [Author and Title](#)

Lin, C.H., Choi, A., and Bennett, R.J. (2011). Defining pheromone-receptor signaling in *Candida albicans* and related asexual *Candida* species. *Mol. Biol. Cell.* 22: 4918–4930.

Google Scholar: [Author Only](#) [Title Only](#) [Author and Title](#)

Liu, R., Chen, Y., Liu, G., Li, C., Song, Y., Cao, Z., Li, W., Hu, J., Lu, C., and Liu, Y. (2020). PI3K/AKT pathway as a key link modulates the multidrug resistance of cancers. *Cell Death Dis.* 11: 797.

Google Scholar: [Author Only](#) [Title Only](#) [Author and Title](#)

Livak, K.J., and Schmittgen, T.D. (2001). Analysis of relative gene expression data using real-time quantitative PCR and the 2^{-ΔΔCT} method. *Methods* 25: 402–408.

Google Scholar: [Author Only](#) [Title Only](#) [Author and Title](#)

Lucas, M.T., and Webster, J. (1964). Conidia of *Pleospora scirpicola* and *P. valesiaca*. *Trans. Br. Mycol. Soc.* 47: 247–256.

Google Scholar: [Author Only](#) [Title Only](#) [Author and Title](#)

Mencke, P., Boussaad, I., Romano, C.D., Kitami, T., Linster, C.L., and Krüger, R. (2021). The role of DJ-1 in cellular metabolism and pathophysiological implications for parkinson's disease. *Cells* 10: 347.

Google Scholar: [Author Only](#) [Title Only](#) [Author and Title](#)

Messiaen, S., Guiard, J., Aigueperse, C., Fliniaux, I., Tourpin, S., Barroca, V., Allemand, I., Fouchet, P., Livera, G., and Vernet, M. (2016). Loss of the histone chaperone ASF1B reduces female reproductive capacity in mice. *Reproduction* 151: 477–489.

Google Scholar: [Author Only](#) [Title Only](#) [Author and Title](#)

Min, Y., Frost, J. M., and Choi, Y. (2020). Gametophytic abortion in heterozygotes but not in homozygotes: implied chromosome rearrangement during T-DNA insertion at the ASF1 locus in *Arabidopsis*. *Mol. Cells* 43: 448–458.

Google Scholar: [Author Only](#) [Title Only](#) [Author and Title](#)

Min, Y., Frost, J.M., and Choi, Y. (2019). Nuclear chaperone ASF1 is required for gametogenesis in *Arabidopsis thaliana*. *Sci. Rep.* 9: 13959.

Google Scholar: [Author Only](#) [Title Only](#) [Author and Title](#)

Mousson, F., Ochsenbein, F., and Mann, C. (2007). The histone chaperone *Asf1* at the crossroads of chromatin and DNA checkpoint pathways. *Chromosoma* 116: 79–93.

Google Scholar: [Author Only](#) [Title Only](#) [Author and Title](#)

Mukherjee, U.A., Ong, S.B., Ong, S.G., and Hausenloy, D.J. (2015). Parkinson's disease proteins: novel mitochondrial targets for cardioprotection. *Pharmacol. Ther.* 156: 34–43.

Google Scholar: [Author Only](#) [Title Only](#) [Author and Title](#)

Nakamura, K., Sakai, S., Tsuyama, J., Nakamura, A., Otani, K., Kurabayashi, K., Yogiashi, Y., Masai, H., and Shichita, T. (2021). Extracellular DJ-1 induces sterile inflammation in the ischemic brain. *PLoS Biol.* 19: e3000939.

Google Scholar: [Author Only](#) [Title Only](#) [Author and Title](#)

Patra, K., Jana, S., Sarkar, A., Mandal, D.P., and Bhattacharjee, S. (2019). The inhibition of hypoxia-induced angiogenesis and metastasis by cinnamaldehyde is mediated by decreasing HIF-1 α protein synthesis via PI3K/AKT pathway. *BioFactors* 45: 401–415.

Google Scholar: [Author Only](#) [Title Only](#) [Author and Title](#)

Prado, F., Cortés-Ledesma, F., and Aguilera, A. (2004). The absence of the yeast chromatin assembly factor *Asf1* increases genomic instability and sister chromatid exchange. *EMBO Rep.* 5: 497–502.

Google Scholar: [Author Only](#) [Title Only](#) [Author and Title](#)

Ramesh, M.A., Malik, S.B., and Logsdon, J.M., Jr. (2005). A phylogenomic inventory of meiotic genes: evidence for sex in *Giardia* and an early eukaryotic origin of meiosis. *Curr. Biol.* 15: 185–191.

Google Scholar: [Author Only](#) [Title Only](#) [Author and Title](#)

Recht, J., Tsubota, T., Tanny, J.C., Diaz, R.L., Berger, J.M., Zhang, X., Garcia, B.A., Shabanowitz, J., Burlingame, A.L., Hunt, D.F., et al. (2006). Histone chaperone *Asf1* is required for histone H3 lysine 56 acetylation, a modification associated with S phase in mitosis and meiosis. *Proc. Natl. Acad. Sci. U S A* 103: 6988–6993.

Google Scholar: [Author Only](#) [Title Only](#) [Author and Title](#)

Saito, H. (2010). Regulation of cross-talk in yeast MAPK signaling pathways. *Curr. Opin. Microbiol.* 13: 677–683.

Google Scholar: [Author Only](#) [Title Only](#) [Author and Title](#)

Sambrook, J.F., and Russell, D.W. (2001). Molecular cloning: a laboratory manual. Cold Spring Harbor laboratory.

Google Scholar: [Author Only](#) [Title Only](#) [Author and Title](#)

Sanematsu, F., Takami, Y., Barman, H.K., Fukagawa, T., Ono, T., Shibahara, K.I., and Nakayama, T. (2006). *Asf1* is required for viability and chromatin assembly during DNA replication in vertebrate cells. *J. Biol. Chem.* 281: 13817–13827.

Google Scholar: [Author Only](#) [Title Only](#) [Author and Title](#)

Scumaci, D., Olivo, E., Fiumara, C.V., La Chimia, M., De Angelis, M.T., Mauro, S., Costa, G., Ambrosio, F.A., Alcaro, S., Agosti, V., et al. (2020). DJ-1 proteoforms in breast cancer cells: the escape of metabolic epigenetic misregulation. *Cells* 9: 1968.

Google Scholar: [Author Only](#) [Title Only](#) [Author and Title](#)

Shao, P., Wang, Y., Zhang, M., Wen, X., Zhang, J., Xu, Z., Hu, M., Jiang, J., and Liu, T. (2019). The interference of DEHP in precocious puberty of females mediated by the hypothalamic IGF-1/PI3K/AKT/mTOR signaling pathway. *Ecotoxicol. environ. Saf.* 181: 362–369.

Google Scholar: [Author Only](#) [Title Only](#) [Author and Title](#)

Simmons, E.G. (1967). Typification of *Alternaria*, *Stemphylium* and *Ulocladium*. *Mycologia* 59: 67–92.

Google Scholar: [Author Only](#) [Title Only](#) [Author and Title](#)

Simmons, E.G. (1969). Perfect states of *Stemphylium*. *Mycologia* 60: 1–26.

Google Scholar: [Author Only](#) [Title Only](#) [Author and Title](#)

Simmons, E.G. (1989). *Macrospora* Fuckel (Pleosporales) and related anamorphs. *Sydowia* 41.

Google Scholar: [Author Only](#) [Title Only](#) [Author and Title](#)

Sitaram, R.T., Cairney, C.J., Grabowski, P., Keith, W.N., Hallberg, B., Ljungberg, B., and Roos, G. (2009). The PTEN regulator DJ-1 is associated with hTERT expression in clear cell renal cell carcinoma. *Int. J. Cancer* 125: 783–790.

Google Scholar: [Author Only](#) [Title Only](#) [Author and Title](#)

Srinivasan, S., Ohsugi, M., Liu, Z., Fatrai, S., Bernal-Mizrachi, E., and Permutt, M.A. (2005). Endoplasmic reticulum stress-induced apoptosis is partly mediated by reduced insulin signaling through phosphatidylinositol 3-kinase/AKT and increased glycogen synthase kinase-3 β in mouse insulinoma cells. *Diabetes* 54: 968–975.

Google Scholar: [Author Only](#) [Title Only](#) [Author and Title](#)

Stajich, J.E., Harris, T., Brunk, B.P., Brestelli, J., Fischer, S., Harb, O.S., Kissinger, J.C., Li, W., Nayak, V., Pinney, D.F., et al. (2012). FungiDB: an integrated functional genomics database for fungi. *Nucleic Acids Res.* 40: 675–681.

Google Scholar: [Author Only](#) [Title Only](#) [Author and Title](#)

Štorchová, H., Hrdličková, R., Chrtek, J., Tetera, M., Fitze, D., and Fehrer, J. (2000). An improved method of DNA isolation from plants collected in the field and conserved in saturated NaCl/CTAB solution. *Taxon* 49: 79–84.

Google Scholar: [Author Only](#) [Title Only](#) [Author and Title](#)

Studt, L., Humpf, H.U., and Tudzynski, B. (2013). Signaling governed by G proteins and cAMP is crucial for growth, secondary metabolism and sexual development in *Fusarium fujikuroi*. *PLoS ONE* 8: e58185.

Google Scholar: [Author Only Title Only Author and Title](#)

Sutton, A., Bucaria, J., Osley, M.A., and Sternglanz, R. (2001). Yeast asf1 protein is required for cell cycle regulation of histone gene transcription. *Genetics* 158: 587–596.

Google Scholar: [Author Only Title Only Author and Title](#)

Taira, T., Saito, Y., Niki, T., Iguchi-Arigo, S.M., Takahashi, K., and Ariga, H. (2004). DJ-1 has a role in antioxidative stress to prevent cell death. *EMBO Rep.* 5: 213–218.

Google Scholar: [Author Only Title Only Author and Title](#)

Teichert, I., Steffens, E.K., Schnaß, N., Fränzel, B., Krisp, C., Wolters, D.A., and Kück, U. (2014). PRO40 is a scaffold protein of the cell wall integrity pathway, linking the MAP kinase module to the upstream activator protein kinase C. *PLoS Genet.* 10: e1004582.

Google Scholar: [Author Only Title Only Author and Title](#)

van der Brug, M.P., Blackinton, J., Chandran, J., Hao, L.Y., Lal, A., Mazan-Mamczarz, K., Martindale, J., Xie, C., Ahmad, R., Thomas, K.J., et al. (2008). RNA binding activity of the recessive parkinsonism protein DJ-1 supports involvement in multiple cellular pathways. *Proc. Natl. Acad. Sci. U S A* 105: 10244–10249.

Google Scholar: [Author Only Title Only Author and Title](#)

Vasseur, S., Afzal, S., Tardivel-Lacombe, J., Park, D.S., Iovanna, J.L., and Mak, T.W. (2009). DJ-1/PARK7 is an important mediator of hypoxia-induced cellular responses. *Proc. Natl. Acad. Sci. U S A* 106: 1111–1116.

Google Scholar: [Author Only Title Only Author and Title](#)

Vasseur, S., Afzal, S., Tomasini, R., Guillaumond, F., Tardivel-Lacombe, J., Mak, T.W., and Iovanna, J.L. (2012). Consequences of DJ-1 upregulation following p53 loss and cell transformation. *Oncogene* 31: 664–670.

Google Scholar: [Author Only Title Only Author and Title](#)

Wang, Q., Wang, S., Xiong, C.L., James, T.Y., and Zhang, X.G. (2017). Mating-type genes of the anamorphic fungus *Ulocladium botrytis* affect both asexual sporulation and sexual reproduction. *Sci. Rep.* 7: 7932.

Google Scholar: [Author Only Title Only Author and Title](#)

Wang, Y., Liu, W., He, X., and Zhou, F. (2013). Parkinson's disease-associated DJ-1 mutations increase abnormal phosphorylation of tau protein through AKT/GSK-3 β pathways. *J. Mol. Neurosci.* 51: 911–918.

Google Scholar: [Author Only Title Only Author and Title](#)

Weng, M., Yang, Y., Feng, H., Pan, Z., Shen, W.H., Zhu, Y., and Dong, A. (2014). Histone chaperone ASF1 is involved in gene transcription activation in response to heat stress in *Arabidopsis thaliana*. *Plant Cell Environ.* 37: 2128–2138.

Google Scholar: [Author Only Title Only Author and Title](#)

Woudenberg, J.H.C., Groenewald, J.Z., Binder, M., and Crous, P.W. (2013). *Alternaria* redefined. *Stud. Mycol.* 75: 171–212.

Google Scholar: [Author Only Title Only Author and Title](#)

Woudenberg, J.H.C., Hanse, B., van Leeuwen, G.C.M., Groenewald, J.Z., and Crous, P.W. (2017). *Stemphylium* revisited. *Stud. Mycol.* 87: 77–103.

Google Scholar: [Author Only Title Only Author and Title](#)

Xu, F., Na, L., Li, Y., and Chen, L. (2020). Roles of the PI3K/AKT/mTOR signalling pathways in neurodegenerative diseases and tumours. *Cell Biosci.* 10: 54.

Google Scholar: [Author Only Title Only Author and Title](#)

Yang, C., Hou, A., Yu, C., Dai, L., Wang, W., Zhang, K., Shao, H., Ma, J., and Xu, W. (2018). Kanglaite reverses multidrug resistance of HCC by inducing apoptosis and cell cycle arrest via PI3K/AKT pathway. *Onco Targets Ther.* 11: 983–996.

Google Scholar: [Author Only Title Only Author and Title](#)

Yang, Y., Gehrke, S., Haque, M.E., Imai, Y., Kosek, J., Yang, L., Beal, M.F., Nishimura, I., Wakamatsu, K., Ito, S. (2005). Inactivation of *Drosophila* DJ-1 leads to impairments of oxidative stress response and phosphatidylinositol 3-kinase/AKT signaling. *Proc. Natl. Acad. Sci. U S A* 102: 13670–13675.

Google Scholar: [Author Only Title Only Author and Title](#)

Yuan, J., Pu, M., Zhang, Z., and Lou, Z. (2009). Histone H3-K56 acetylation is important for genomic stability in mammals. *Cell Cycle* 8: 1747–1753.

Google Scholar: [Author Only Title Only Author and Title](#)

Zhang, C., Ren, X., Wang, X., Wan, Q., Ding, K., and Chen, L. (2020). FgRad50 regulates fungal development, pathogenicity, cell wall integrity and the DNA damage response in *Fusarium graminearum*. *Front. Microbiol.* 10: 2970.

Google Scholar: [Author Only Title Only Author and Title](#)

Zhang, Y., Gong, X.G., Wang, Z.Z., Sun, H.M., Guo, Z.Y., Gai, C., Hu, J. H., Ma, L., Li, P., and Chen, N.H. (2016). Protective effects of DJ-1 mediated AKT phosphorylation on mitochondrial function are promoted by Da-Bu-Yin-Wan in 1-methyl-4-phenylpyridinium-treated human neuroblastoma SHSY5Y cells. *J. Ethnopharmacol* 187: 83–93.

Google Scholar: [Author Only Title Only Author and Title](#)

Zhao, Y., He, M., Ding, J., Xi, Q., Loake, G.J., and Zheng, W. (2016). Regulation of anticancer styrylpyrone biosynthesis in the medicinal mushroom *Inonotus obliquus* requires thioredoxin mediated transnitrosylation of S-nitrosoglutathione reductase. *Sci. Rep.* 6: 37601.

Google Scholar: [Author Only](#) [Title Only](#) [Author and Title](#)

Zhou, X., Li, G., and Xu, J.R. (2011). Efficient approaches for generating GFP fusion and epitope-tagging constructs in filamentous fungi. *Methods Mol. Biol.* 722: 199–212.

Google Scholar: [Author Only](#) [Title Only](#) [Author and Title](#)

Zhou, Y., Li, S., Li, J., Wang, D., and Li, Q. (2017). Effect of microRNA-135a on cell proliferation, migration, invasion, apoptosis and tumor angiogenesis through the IGF-1/PI3K/AKT signaling pathway in non-small cell lung cancer. *Cell. physiol. Biochem.* 42: 1431–1446.

Google Scholar: [Author Only](#) [Title Only](#) [Author and Title](#)

Zhu, Y., Weng, M., Yang, Y., Zhang, C., Li, Z., Shen, W.H., and Dong, A. (2011). Arabidopsis homologues of the histone chaperone ASF1 are crucial for chromatin replication and cell proliferation in plant development. *Plant J.* 66: 443–455.

Google Scholar: [Author Only](#) [Title Only](#) [Author and Title](#)